Recycling of Lithium Iron Phosphate (LiFePO<inf>4</inf>) Batteries from the End Product Quality Perspective

batteries

MDPI

Review

Recycling of Lithium Iron Phosphate ($LiFePO_4$) Batteries from the End Product Quality Perspective

Deise F. Barbosa de Mattos, Simon Duda * and Martina Petranikova *

Nuclear Chemistry and Industrial Materials Recycling, Chalmers University of Technology, Kemivägen 4, SE-412 58 Göteborg, Sweden; deiseb@chalmers.se

* Correspondence: simond@chalmers.se (S.D.); martina.petranikova@chalmers.se (M.P.)

Abstract: As efforts towards greener energy and mobility solutions are constantly increasing, so is the demand for lithium-ion batteries (LIBs). Their growing market implies an increasing generation of hazardous waste, which contains large amounts of electrolyte, which is often corrosive and flammable and releases toxic gases, and critical raw materials that are indispensable to the renewable energy sector, such as lithium. Therefore, it is crucial that end-of-life LIBs be recycled in a viable way to avoid environmental pollution and to ensure the reuse of valuable materials that would otherwise be lost. Here, we present a critical review of recent developments in the field of LIB recycling with the $LiFePO_4$ (LFP) chemistry, which is one of the fastest-growing fields, especially in the electromobility sector. Most of the recycling methods developed are not applied industrially due to issues such as complexity, cost, or low quality of the recycled product. This last issue is rarely discussed in the literature, which motivated the creation of this review article, with emphasis on the positive electrode recycling by the direct method and on the quality of the resynthesized LFP in terms of electrochemical performance.

Keywords: battery recycling; direct recycling; Li-ion batteries; $LiFePO_4$; LFP

Academic Editor: George Zheng Chen

Received: 5 December 2024
Revised: 12 January 2025
Accepted: 13 January 2025
Published: 18 January 2025

Citation: Barbosa de Mattos, D.F.; Duda, S.; Petranikova, M. Recycling of Lithium Iron Phosphate ($LiFePO_4$) Batteries from the End Product Quality Perspective. *Batteries* **2025**, *11*, 33. https://doi.org/10.3390/batteries11010033

1. Introduction

Since 2015, nearly 200 countries have committed to taking action to limit climate change and its impacts, driven by the need to reduce greenhouse gas emissions by increasing the use of renewable energy sources for electricity, heating, and transportation [1]. The challenge to accomplish this is energy storage. Unlike fossil fuels, which are easily stored to harness the energy contained in their chemical bonds through burning, renewable sources—including wind, solar, and hydroelectric power—require that the converted energy be stored in batteries or chemical compounds such as hydrogen [2,3].

The lithium-ion battery (LIB), developed in the early 1990s, has been enabling progress towards increased renewable energy conversion. Basically, a battery is made of electrochemical cells. The cells contain two electrodes and an electrolyte. The negative electrode (also referred to as anode) is made with an element that easily releases electrons from its valence shell. The positive electrode (also referred to as cathode) receives electrons from the negative electrode through an external circuit. The potential difference between the electrodes results in cell voltage. Therefore, at the anode, an oxidation reaction takes place, and at the cathode, there is a reduction of the species that is carrying the charge through the electrolyte. The electrolyte is the medium through which the cation, which has lost its electron on the negative electrode, moves to the positive electrode in the discharging process. A barrier separates and prevents physical contact between the electrodes so that the battery does not short-circuit [4–7].

Lithium is the first solid element on the periodic table and the lightest metal. It contains only one electron in the valence shell, which can be easily removed (Li^+/Li reduction potential is −3.04 V vs. SHE) [8]. Lithium metal is reactive in contact with water and air; therefore, the electrodes are made by intercalation, in which a solid contains atomic vacancies where lithium ions can enter and leave. The first LIBs were developed with a lithium cobalt oxide cathode active material (CAM) ($LiCoO_2$—in short LCO). The demand, price, and uneven distribution of cobalt in the world has caused the price of the battery to increase. The development of other types of positive electrodes, such as $LiNixCoyMnzO_2$ (NMC), $LiNi_{0.8}Co_{0.15}A_{l0.05}O_2$ (NCA), and $Li_2Mn_2O_4$ (LMO), has allowed not only a reduction in cost but also better performance [9–12]. The chemical composition of the electrode results in batteries with different efficiencies in specific energy density, specific power, lifetime, and performance. For example, in terms of the specific energy density, that is, the amount of energy that a battery stores per unit mass, NCA and NMC have the best performance, with 200–260 Wh/kg and 150–220 Wh/kg, respectively [4,13,14].

In the mid-1990s, iron-based CAMs were developed to reduce the price of batteries to be used in electric vehicles (EVs) [6,12]. Iron is an abundant, cheap, and non-toxic metal. Good rechargeability and high open circuit voltage were obtained in lithium–iron–phosphate electrodes ($LiFePO_4$—in short LFP). The ordered olivine structure of LFP (Figure 1a) allows for extraction and insertion of the lithium ion (Li^+) during cell discharge and charge, maintaining the same framework. De-intercalation of lithium results in iron phosphate (FePO4), changing the iron oxidation state from Fe^{2+} to Fe^{3+} [12,15,16]. Although a lower specific energy density (90–120 Wh/kg) is obtained, LFP has the best safety performance [4,13,14].

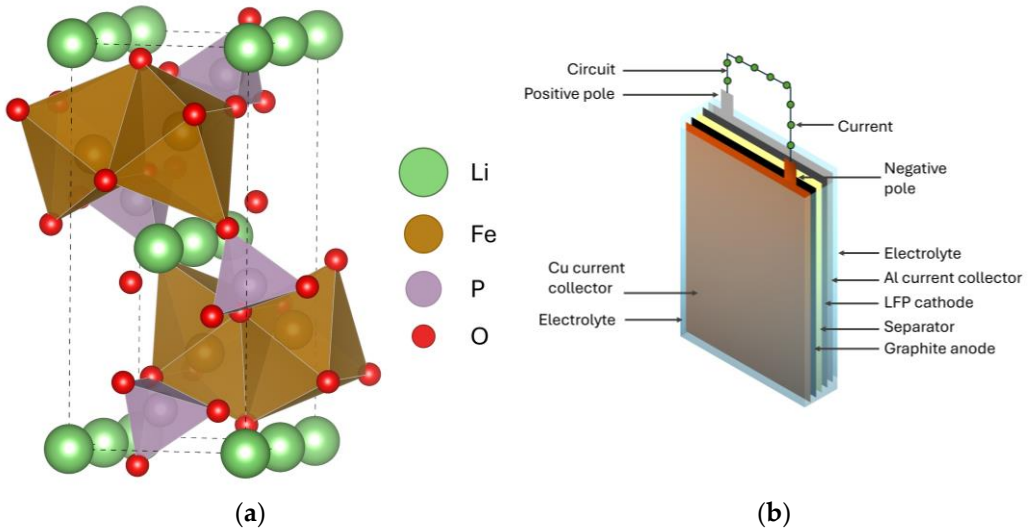

(**a**) (**b**)

Figure 1. Illustration of (**a**) LFP crystalline material made using VESTA software version 3.90.1a [17] and (**b**) the construction of a single LFP battery cell.

Basically, the preparation of the LFP electrode consists of mixing the compounds that serve as a source of iron, phosphate, and lithium and carbon coating. Then, the mixture is sintered at a high temperature in an inert atmosphere to avoid the formation of Fe^{3+}. The $LiFePO_4$ is cast on an aluminum foil (Al), which is the current collector, using a binder, which is often polyvinylidene fluoride (PVDF) [10,18,19]. The development of a carbonaceous anode made the LIBs pass safety tests [4,6,20]. In the negative electrode, lithium is intercalated in graphite (which has a potential close to metallic lithium) and cast on copper foil (Cu) as a current collector. Usually, a polymer, Teflon, or carboxy methyl cellulose (CMC) is used as a anode binder [4,8,21–24]. To complete the LFP electrolytic cell,

the electrolyte mainly used is lithium hexafluorophosphate ($LiPF_6$), in an alkyl carbonate solvent, and the separator is a microporous polymeric film [4,6,25]. Figure 1b illustrates the schematic assembly of the LFP battery. During discharge, lithium de-intercalates from the negative electrode (Equation (1)). Li^+ is transported through the electrolyte and intercalates in the positive electrode (Equation (2)) [4,12].

$$Li_xC_6 \rightarrow xLi^+ + xe^- \quad (1)$$

$$FePO_4 + xLi^+ + xe^- \rightarrow xLiFePO_4 + (1-x)FePO_4 \quad (2)$$

With this configuration, the LFP cell is cheap, safe, and chemically and thermally stable (can withstand up to 270 °C), does not release oxygen at high temperature (minimizing the risk of electrolyte combustion), has a flat voltage profile and high cycling performance (1000 to 2000 cycles of charge-discharge), and results in a high potential of 3.5 V [6,9,11,12,15,18,26]. A factor to be improved is its reduced performance at low temperatures [27–29]. For all its good performance, finally in 2020, LFP became the main battery for EVs, placing LIB for its conceptual purposes, which were the reduction of harmful exhaust gases from cars and overcoming the oil crisis [30,31].

Although the large-scale use of LFP contributes to the progress in reducing greenhouse gas emissions, a new concern arises related to the growing demand for lithium extraction and the generation of electronic waste. Therefore, it is necessary for responsible consumption and production of natural resources, with reduction of waste by preventing its generation and facilitating recycling [1]. By 2030, around 140 million EVs are expected to be on the streets, and this will generate 11 million tons of used batteries. Considering that the lifespan of an LIB is 10 to 15 years, it is urgent that strategies be applied to delay disposal, establish second-use applications, or recycle [32].

The concern about recycling LIBs comes simultaneously from its initial development, making it necessary to recover expensive metals with limited availability [33]. Additionally, batteries are classified as hazardous waste; when discarded, there is a high risk of fire associated with its degradation [25]. Although the LFP battery is based on iron, which is an abundant and low-value natural resource, recycling should not be postponed so as to avoid waste stock and reduce mining, which in turn has a major environmental impact [25,34]. Another important point for LFP battery elements is that lithium, phosphorus, and copper are listed as critical raw materials for the European Union (EU). To ensure that the EU has a sustainable supply of these materials, the recycling capacity should be 25% of their annual consumption by 2030 [35]. According to EU 2023/1542 regulation for batteries, by 2036, industrial batteries with a capacity greater than 2 kWh must be manufactured with 12% lithium from recycling, and the processes should reach, by 2030, a lithium recycling and recovery efficiency of 70% and 80%, respectively [36].

The LIB is used in EVs until its capacity falls to 70–80% of the nominal one [37]. When the battery no longer meets the requirements for use in EVs, it can still be used in applications with lower demands and enter the so-called second-life use. These batteries are evaluated for various performance and safety requirements, and they are repurposed in fixed-station energy storage systems, such as residential buildings, uninterruptible power supply, or storage of energy from renewable sources [38–41]. Monitoring battery health is important to define when it is no longer sufficient for second-life activities. Then, it must be destined for correct disposal or recycling.

Even though the battery has a long life, the complex physicochemical mechanisms that occur in the LFP electrochemical cell lead to its degradation, making it lose its charging capacity. The $LiFePO_4$ and $FePO_4$ phases have the same crystalline structure; however, during lithiation and delithiation, volume changes and edge displacement effects cause stress

on the structure, forming inactive trigonal $FePO_4$, and mechanical degradation [12,42]. Also, during the charge and discharge cycle, over time, there are physical changes on the surface of the LFP electrode, increasing its resistance. This occurs due to the coarsening of LFP particles and loss of carbon coating [43]. The electrolyte reacts with the electrode surface, forming a solid electrolyte interface (SEI). It is a passivating layer, which is insoluble and protective, minimizing electrode decomposition. However, if the thickness of this layer is large, the Li^+ diffusion channels are blocked, inhibiting its transport to the electrode [8,44–48]. Other degradation pathways are related to the loss of lithium mass and decomposition of the PVDF binder [49]. An advantage of the LFP battery is that it does not release oxygen at elevated temperatures, which is very harmful to the positive electrode and raises concerns about battery safety in oxide-based CAMs [50].

Ideally, LFP recycling should be in a cycle that allows for reuse of the CAM in the manufacture of new batteries. An important parameter to be considered in the resynthesis of LFP using recycled material is the battery performance, which is determined by its specific energy density; its capacity (denoted as Cn or C/n, with unit of Ah), which is the current provided by the battery and the time, n, for complete discharge; and cycling ability, which is the number of charge–discharge cycles without performance loss [4]. For LFP batteries, the cycling ability is 1000–2000, and the typical specific capacity (SC) is 120–160 mAh/g [4,13,51].

Generally, the routes used for recycling are pyrometallurgy, hydrometallurgy, or a combination of both, and direct CAM regeneration. The choice of method depends on the CAM chemistry and economic viability. In the case of LFP, which has low added value, the challenge of a recycling process arises. Many research efforts in the recycling of LFP have been made, but are yet to be industrially applicable. For researchers to understand the course of the development and what to focus on in their own work, updated systematic reviews are important. Present review papers describe the currently reported recycling strategies mainly in terms of their functionality and principles, focusing on economic and environmental aspects in their comparisons. However, should the strategies be implemented industrially, an overview of the quality and performance of the recycled products will be necessary to determine the most promising technology. Despite its apparent importance, this aspect is only scarcely discussed in the present literature. This paper mainly reviews LFP CAM recycling routes based on the direct method, which tends to be a cheaper method than pyro- and hydrometallurgy, as it is performed in fewer steps. Emphasis is placed on the quality of the final resynthesized LFP CAM in terms of specific capacity.

2. Handling and Mechanical Pre-Treatment of Spent Batteries

Before starting the recycling process, the battery needs to be collected and classified according to its chemical composition, to decide which is the most viable recycling route. Pyro- and hydrometallurgical recycling processes are the most used nowadays. In the case of LFP, whose elements do not have much commercial value, recycling becomes expensive. To overcome it, there is the possibility of direct recycling to reduce the processing steps or to use the same process line for recycling batteries with mixed chemistry. Depending on the quality of the final product, it is used in the production of a new positive electrode [52–55] and other chemicals for applications such as water treatment [56,57], catalysts [58], and fertilizers [59]. Great care must be taken in the production of a new electrode because the presence of impurities in the chemistry of lithium batteries is responsible for causing internal failures, which is a safety risk in using batteries [60].

After the collection and classification of batteries regarding their chemical composition and by testing their state of health to confirm that they have reached the end-of-life, the pre-treatment for recycling begins. Frames, cables, and main electronic circuits are removed.

It is necessary to discharge the residual charge of the battery before starting to disassemble its parts. Then, each part, which constitutes the battery, plastic, metal, electrolyte, and electrodes, is separated and the black mass or the active material of the electrodes is obtained (Figure 2).

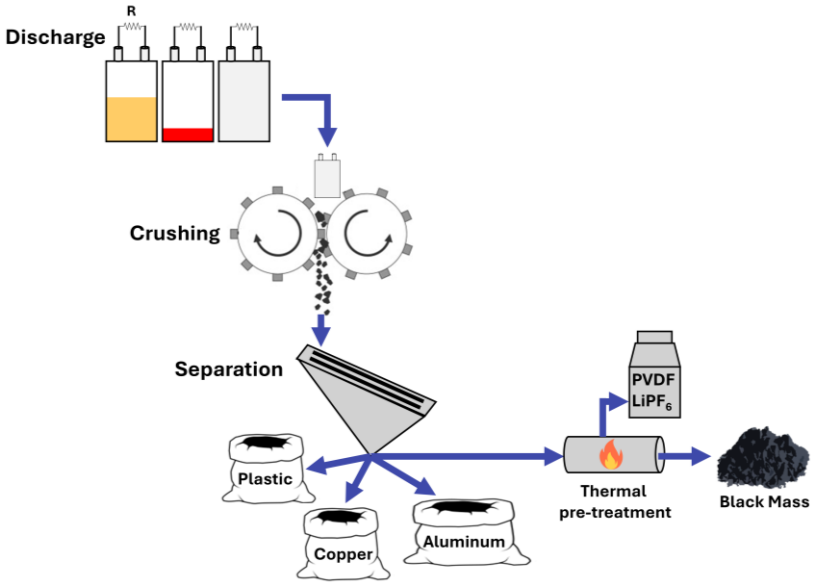

Figure 2. Illustration showing the operations required to prepare the black mass.

2.1. Battery Discharge and Dismantling

An important step is the complete discharge of batteries to ensure safety during comminution [61]. The electrolyte solvent, the possibility of the electrodes coming together, and the formation of volatile organic compounds can cause fire and explosion [62–66]. Discharging can be performed in a controlled manner in an external circuit with resistance or in a saltwater bath [64–68]. The latter allows for discharge on a large scale; however, it causes corrosion and contamination in the recycling process [67–69].

2.2. Mechanical Processing and Separation

Once the battery is fully discharged, it is sent to the crushing procedure. The battery is shredded and the metallic parts of the aluminum casing, the copper and aluminum foils from the negative and positive electrode, respectively, and the plastic parts are separated using sieves and magnetics [62]. The shredding stage is usually carried out in a controlled atmosphere with inert gas to prevent lithium reactions and the escape of toxic gases that can be formed from the electrolyte [25,70].

The material that is left is finely crushed, and it is the so-called black mass. The mass contains the valuable elements of the cathode, and the black color comes from the graphite in the anode. Other materials, such as the binder, electrolyte, and small fragments of metals and plastic, are still present [25,62].

2.3. Black Mass Thermal Pre-Treatment

This step involves removing the electrolyte, the electrode materials that are still bound to the aluminum and copper foils, and finely ground metals, such as aluminum, from the battery outer shell [25,71].

Usually, thermal decomposition of $LiPF_6$ electrolyte is applied; however, it forms corrosive and toxic gases such as hydrofluoric acid and phosphorus pentafluoride (PF_5) [72–81]. To avoid toxic gas formation, other types of treatments are recommended in the literature, such as solvent extraction [77,82–84], fractional distillation and selective peeling [85],

supercritical carbon dioxide (CO_2) [73,86,87], and ultrasonic-assisted acid peeling [88]. These methods show good results in the laboratory; however, for them to be applied in the industry, toxicity, cost, and practicality on a large scale must be considered. In general, thermal pre-treatment can be performed before or after mechanical separation.

2.4. Removal of Aluminum and Copper Current Collectors

The presence of Cu and Al increases acid consumption in hydrometallurgical processes. Furthermore, they negatively affect the electrochemical performance, lifetime, and stability of positive electrodes synthesized with recycled LFP material [60,89,90]. Therefore, an efficient separation between the active materials of the electrodes and the current collectors prior to black mass formation is advantageous. Mechanical methods use the differences between the properties of electrode active material, Al and Cu, such as color and conductivity. The reported recovery for these methods is around 90% for metallic foils and between 50 and 99% for electrode material [91–93]. Another option is to liberate the metal foils by removing the PVDF binder by thermal degradation at 550 °C. Although more than 97% of the active material of the electrodes can be recovered, there is release of toxic gases such as hydrofluoric acid (HF), hydrogen cyanide (HCN), and carbon monoxide (CO) [94–99]. To avoid high temperatures, Al and Cu can be dissolved with concentrated sodium hydroxide or with concentrated acid leaching, followed by solvent extraction and precipitation, or alkaline carbon adsorption, to remove them later. In these cases, a recovery of 99% is obtained; however, these methods require a large amount of solution to be treated for disposal or recycling [53,71,100,101].

2.5. Methods Applied in the Direct Recycling Approach

The recycling of black mass commonly applies pyro- and hydrometallurgy methods. However, to reduce the energy required in the former and the amount of reagents in the latter, direct recycling has been developed to recover and re-synthesize the positive electrode. For that, careful disassembly of the battery and individual removal of the current collectors is advantageous because the respective electrodes need to be treated separately without the formation of the black mass.

Within the direct recycling realm of LFP recycling research, the CAM is separated from the aluminum current collector mostly by deactivation of the PVDF binder by hydrolysis. Often, it is reported that hydrolysis is preceded by washing the positive electrode with dimethyl carbonate to remove electrolyte residues [96,102–104]. After the separation, filtration, and drying, the material is ground, or alternatively ball-milled [98,103], to obtain pure CAM in a dry powder form.

Another approach is to remove the PVDF binder of the positive electrode and maintain the structure of the current collector. This can be achieved by applying force, such as ultrasound cleaning and ball milling, or cryogenic grinding [96,102,105–109]; by dissolution in organic solvents, commonly N-methyl pyrrolidone (NMP) [83,110–112], sodium hydroxide [103], or fatty acid methyl ester [113]; by aluminum passivation with concentrated sulfuric or phytic acid [114,115]; by competitive binding with ethylene glycol [116]; or by cooling and freeze drying [117]. Using these methods, it is possible to achieve close to 100% recovery for both current collector foils and CAM.

The binder of the graphite anode is usually a water-soluble adhesive, and it can be easily separated from copper foil through scraping or sonication [54,92,105,118–121].

2.6. Removal of Graphite

The reported method of removing graphite from the black mass is mainly based on flotation due to its hydrophobicity, while LFP is hydrophilic. It is reported that the LFP recovery efficiency using this technique varies from 50 to 96%, depending on the

parameters used in the operation and whether there is a thermal pre-treatment of the black mass [93,122–124]. Another possibility is to use a magnetic separator, as graphite is diamagnetic and LFP is paramagnetic. In this case, the reported LFP recovery can reach 98% [125]. Removing graphite from the black mass facilitates the leaching stage if the hydrometallurgical process is subsequently used to separate the cathode elements, because it reduces foam formation in the reactor.

3. Recycling Technologies

3.1. Pyrometallurgy

In pyrometallurgy, a high temperature (>600 °C) is used to separate metals. By varying the temperature phase transitions, lattice changes and chemical reactions occur. The process usually involves the steps of pyrolysis and smelting under an inert atmosphere (Figure 3). Therefore, it depends on the temperature, processing time, type of purge gas, and flux addition [25,126–129].

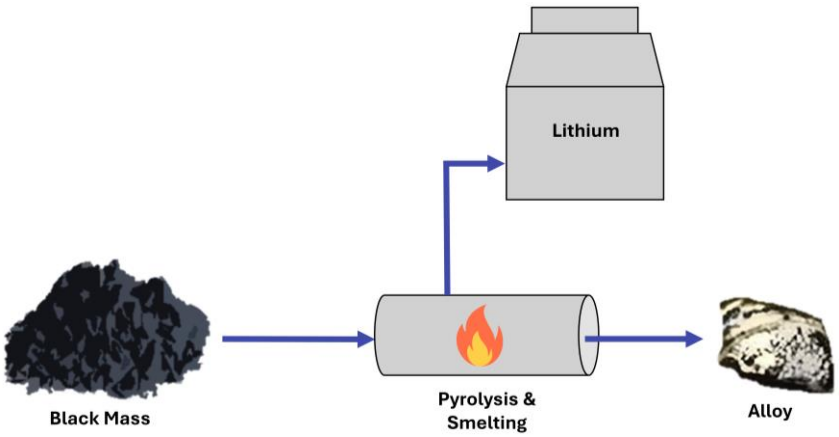

Figure 3. Schematic illustration of the pyrometallurgy recycling route.

During pyrolysis, organic material is decomposed. For LFP, the PVDF binder is removed at 550 °C, followed by carbon black and graphite at 650 °C. There is formation of hazardous gases, such as HF, hydrogen cyanide (HCN), and CO_2 [95,130]. During smelting, the temperature is raised to the melting points of cathodic metals (around 1000 °C). While lithium is volatilized, iron is reduced and concentrated together with phosphorus into an alloy. A slag is formed containing phosphorus and some iron oxides that are not reduced [131,132]. Qu et al. reported 95.5% volatilization for lithium, which was then recovered in water. They also obtained 98.9% and 92.1% recovery for iron and phosphorus; however, almost 20% of iron also volatilized [132].

Inorganic salts can be added to the black mass to form carbonates and alkali metal halides (sodium carbonate, calcium chloride, sodium hydroxide) and help in the capture of the elements and decrease the smelting temperature (to around 200 °C) [126,133,134]. Li et al. used NaOH to oxidize Fe^{2+} at 150 °C and release Li^{+} from the olivine structure, followed by leaching in water. The lithium recovery reached 96.7% [133].

Recycling LFP batteries through pyrometallurgy is advantageous due to its simplicity and the low aggregated value of cathode materials. It was observed that heat treatment in $LiFePO_4$ results in recycled electrodes with a specific capacity higher than 110 mAh/g [34,135,136]. Pyrometallurgy allows for high production capacity, and no pre-treatment of the black mass is necessary. A mixture of different lithium batteries can be processed, and it can be accomplished in a short time and is a solvent-free process. On the

other hand, there is high energy consumption, toxic gases formation, and metal losses, and additional purification of the alloy is necessary [126,128,132,137].

3.2. Hydrometallurgy

In hydrometallurgy, the metals in the black mass are dissolved in water using acids or bases (Figure 4). Afterwards, oxidation, sedimentation, separation, and purification steps are necessary to separate the elements, which are obtained as hydroxide or metal salt. The efficiency of the process depends on the leaching agent concentration, pH, temperature, time, stirring speed, particle size, solid–liquid ratio, and oxidizing agent concentration [26,138–140]. Unlike pyrometallurgy, the leaching process is carried out at a low temperature (<90 °C) and there is low energy consumption [26,139]. However, there is a large volume of aqueous effluent that requires treatment.

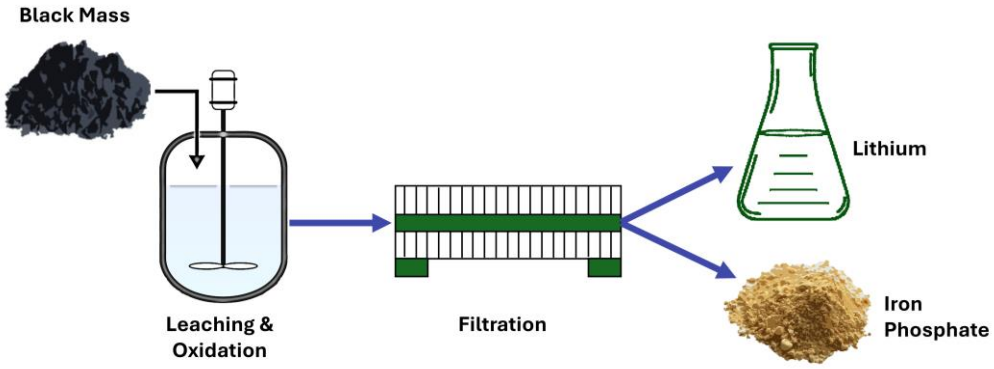

Figure 4. Schematic illustration of the hydrometallurgy recycling route.

When strong acids (sulfuric, phosphoric, nitric) are used to completely solubilize the cathode elements, the olivine structure of LFP is destroyed, and then lithium, phosphorus, and iron enter the solution. Afterwards, lithium is recovered using a precipitation agent. Finally, an oxidizing agent, usually hydrogen peroxide (H_2O_2), is used to oxidize Fe^{2+} to Fe^{3+} and it precipitates with phosphorus. A disadvantage of this method is that a large volume of reagents is necessary. To overcome this, the leaching and oxidation steps can be performed together using weak acids (formic, citric) or neutral conditions. Lithium is selectively leached when iron in the olivine structure is oxidized. The solid structure of LFP changes its lattice and $FePO_4$ precipitates. The solid residue is separated through filtration, a precipitating agent is added to the solution, and lithium is obtained as carbonate, hydroxide, or phosphate [129,141–145].

Both complete and selective leaching can be performed using the same acid and changing pH. For example, sulfuric acid (H_2SO_4) was used to perform the leaching of $LiFePO_4$ (Table 1). Zheng et al. thermally treated the cathode at 600 °C to remove the binder and oxidize iron. After complete acid leaching, ammonia was used to change the pH and precipitate amorphous hydrated $FePO_4$. Finally, sodium carbonate (Na_2CO_3) was added to the filtrate to precipitate lithium carbonate (Li_2CO_3) [138]. Li et al. pre-treated the electrode with sodium hydroxide solution under ultrasound to separate the LFP from the aluminum foil. Selective acid leaching and oxidation were performed together, with H_2O_2 as the oxidizing agent (H_2O_2/Li molar ratio 2.07). Lithium was precipitated as $LiPO_4$ using sodium phosphate dodecahydrate [139]. The authors point out that when pH decreases, iron enters the solution. The optimal value of pH, to not leach iron, was also reported by Jin et al., who used air as an oxidant (flow rate = 600 mL/min) and recovered lithium as Li_2CO_3 [55].

Table 1. Reported experimental conditions used for complete and selective leaching of LFP with sulfuric acid; liquid–solid ratio (L/S), temperature (T).

Leaching	H_2SO_4 Concentration [M]	L/S [mL/g]	pH	T [°C]	Leaching Efficiency [%]			Ref.
					Li	Fe	P	
Complete	2.5	10.0	1.5	60	97.0	98.0	-	[138]
Selective	0.3	10.5	3.7	60	95.7	0.017	1.97	[139]
Selective	9.0	10.0	3.5	25	99.3	0.020	0.020	[55]

3.3. Direct Recycling

Unlike in pyro- and hydrometallurgical technologies, where the product normally comprises the constituent metals from the battery in various forms, such as alloys or metal salts, the aim of direct recycling is to regenerate (mostly) the positive electrodes, preferably to virgin performance. Other parts of the batteries could in theory be directly regenerated as well; however, with their much lower economic value compared to the cathodes, the incentives for this are not high. Thus, research has mainly focused on the direct regeneration of cathodes. Presently, direct recycling is still in the research or pilot phase owing to several challenges with industrial application, as discussed later. Figure 5 shows a flow chart of the way direct recycling theoretically functions, i.e., as a loop of battery usage and recycling, where the CAM is constantly regenerated and reused.

Figure 5. Illustration of the direct recycling flow scheme.

Before the regeneration begins, the batteries are discharged and dismantled to obtain individual cells. These are then opened to harvest individual cathode and anode sheets, while the electrolyte evaporates. The discharging and dismantling processes are rarely given any attention in the literature. Most of the reported regeneration strategies require CAMs to be separated from the aluminum current collector foil, as discussed previously.

After separation, one can, so far, identify six main categories of regeneration routes, namely hydrothermal, molten salt assisted, solid-state thermal, electrochemical, chemical, and indirect regeneration. The last one differs from the rest in that it starts with hydrometallurgical treatment. Then, instead of purifying and selling the products to other applications, one attempts to use them directly in the production of new CAMs. We chose to call this approach "indirect direct recycling". In the following sections, each route is described in terms of work principles and the current state of research, followed by a comparison of the

routes and their advantages and disadvantages. Note that the electrochemical performance of the produced electrodes is not always reported in the text. For data on all the examined papers, please refer to Tables 2 and 3, where the best claimed performance is presented.

3.3.1. Solid-State Thermal Regeneration

Perhaps the most extensively researched direct recycling route, along with the indirect approach, is solid-state thermal regeneration. As the name suggests, this method means regenerating CAMs with the help of heat. Generally, defective LFP is mixed with a stoichiometrically accurate amount of a Li salt, and then thermally treated at several hundred °C in a reductive environment for sintering/calcination [146]. Figure 6 shows a general flow scheme for the solid-state thermal regeneration technique.

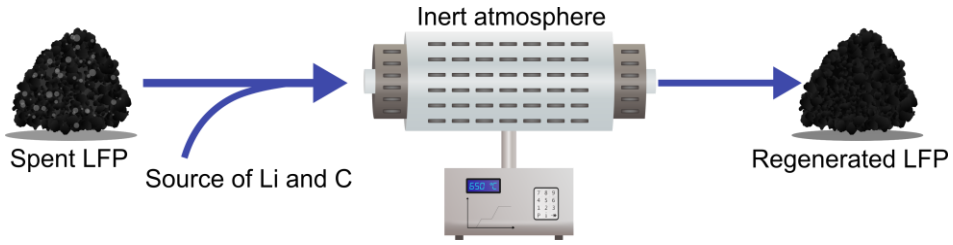

Figure 6. Illustration of the general solid-state thermal regeneration technique.

The main advantages of this method are its simplicity and a relatively small number of steps, as well as minimized need for chemicals [108,147,148]. Also, if potential industrialization is regarded, it is important to note that the industries are likely to prefer a dry LIB recycling method over a wet one, especially due to the enhanced risk of HF formation from electrolyte and binder residues in contact with water [149].

However, the generation of toxic gases that end up in the exhaust stream is also an issue for solid-state thermal regeneration. Moreover, it suffers from difficulties in ensuring uniform (a) distribution of the added Li^+ in the regenerated CAM and (b) crystallinity and suitable morphology of the repaired LFP particles [96,102,103,150]. This poses a challenge for a possible industrial application, as spent batteries come in a large variety of degradation states. For that same reason, it is difficult to determine the exact appropriate amount of Li source that should be added to a batch of CAMs from different batteries, matching the amount of missing active Li [102]. Another disadvantage is the high energy consumption connected to the use of high temperatures for extended periods of time [147].

Before a method that falls under this category can be implemented industrially, research needs to address the issues related to it. In fact, many researchers have tackled these challenges in the last decade. Starting in 2016, Chen et al. demonstrated the effects of heat treatment under an inert atmosphere (Ar/H_2) at different temperatures. They showed that a higher temperature reduces the particle agglomeration in the cathode powders, allowing for increased discharge capacities, while too high temperatures may lead to decomposition of the LFP particles, decreasing the discharge capacity of the recycled CAM. Ultimately, they found that a temperature of around 650 °C is optimal for obtaining a recycled cathode powder with the highest discharge capacities [151].

This paved the way for further research in thermal regeneration. Song et al. took a similar approach to the regeneration process while sintering under N_2 atmosphere and doping the spent cathode powders with pristine LFP powders during sintering at different temperatures and spent/pristine doping ratios. The best results were obtained after sintering at 700 °C with a doping ratio of 3:7, achieving an improvement in the electrochemical performance after electrochemical testing, compared to Chen et al. [112,151]. Further improvements were achieved by Li et al., who regenerated scrapped LFP by

calcination in the presence of lithium carbonate (Li_2CO_3) at different temperatures under argon (Ar) or hydrogen (H_2) flow. Aligned with the previous results, the best performance of the regenerated CAMs was measured after calcination at 650 °C [152].

Liang et al. took a slightly more involved approach to direct regeneration, with multiple heat treatment steps. After an initial sintering at 450 °C under air for purification purposes, the clean LFP powders were complemented with stoichiometric amounts of undisclosed Li/Fe/P salts, and then ball-milled and spray-dried between 220 °C and 120 °C. One final sintering treatment was done at 650 °C under N_2, ultimately achieving a slightly lower performance of the repaired LFP of 139 mAh/g at 0.2 C, compared to Li et al., with 147.3 mAh/g at 0.2 C [152,153].

So far, researchers have mostly performed thermal regeneration of spent LFP by the addition of a suitable amount of Li salt. It was shown, however, that the inclusion of a carbon source in the reaction, such as glucose, is beneficial. The purpose is dual—carbon promotes the reduction of Fe^{3+} to Fe^{2+}, thus facilitating material regeneration. Moreover, coating of the LFP with carbon, as a result of the high-temperature treatment, has been shown to increase the conductivity of the material [154]. This was implemented by Chen et al., who regenerated spent LFP electrodes in the presence of Li_2CO_3 and glucose by a two-step roasting process at 350 °C for 4 h, followed by 650 °C for 9 h [107]. Later, Qi et al. combined this with Liang's initial annealing to remove residues of PVDF, carbon, and electrolyte [99,153]. Then, Li_2CO_3 and glucose in different ratios were mixed with the purified LFP powders using ball milling, followed by a two-step heat treatment at 350 °C for 2 h, and then 900 °C for 6 h, achieving 96% recovery in specific discharge capacity compared to pristine LFP [99]. Li et al. continued the same approach, but performed the first annealing step under air, thus carrying out a pre-oxidation reaction. Furthermore, they incorporated nano-sized titanium dioxide as doping in the second annealing reaction, along with Li_2CO_3 and glucose. They found that a 1% doping with titanium can significantly improve the electrochemical properties of the regenerated LFP, for instance, by increasing the initial discharge capacity from 144.1 mAh/g to 147.3 mAh/g, with the difference further increasing later in the measurements [154].

Similar strategies, but with extra added reaction agents for enhanced electrochemical properties, were pursued. Song et al. employed activated carbon nanotubes (CNTs), along with Li_2CO_3 and glucose. CNTs are thought to enhance the ionic conductivity of the regenerated LFP, owing to their three-dimensional nanostructure. After ball-milling in an ethanol–water mixture, then drying and annealing at 350 °C for 2 h and 650 °C for 12 h under Ar, an impressive recovery of the specific discharge capacity of ~99% vs. pristine LFP was accomplished [109]. Using an almost identical process and reaction parameters, Yao et al. exchanged the CNTs for Cu doping using cupper nitrate hydrate, $Cu(NO_3)_2{\cdot}2.5\ H_2O$, reaching slightly lower capacity recovery than Song et al., but an excellent capacity retention of 81% over 1000 cycles at a 1 C discharge rate [108].

Li salts other than Li_2CO_3 have been studied in thermal regeneration processes. Recently, Ji et al. managed to bypass the addition of an extra reducing agent and carbon source to the regeneration reaction by using a multifunctional organic lithium salt, namely 3,4-dihydroxybenzonitrile dilithium (Li_2DHBN). They showed that the salt couples with the surface of the spent LFP, and that upon regeneration, it serves three purposes: (a) high temperature facilitates the transport of Li^+ into the empty sites, (b) the cyano groups act as a reducing agent, and (c) the amorphous carbon formed upon pyrolysis of the Li_2DHBN creates a coating layer on the LFP particles. The regeneration was done by sintering the spent LFP and Li_2DHBN at 800 °C for 6 h under Ar/H_2, achieving the best overall electrochemical performance of the three salts that were investigated in this study, the other two being Li_2CO_3 and lithium hydroxide (LiOH). For comparison, the electrode regenerated

with Li_2DHBN reached an initial discharge capacity of 111 mAh/g at 5 C, while the ones regenerated with the inorganic salts only reached 73 and 77 mAh/g, respectively, at the same current density. Moreover, the capacity retentions were reported as 88%, 78% and 76%, respectively, after 400 cycles under the same conditions [155].

3.3.2. The Molten Salt Approach

Almost a subset of the thermal regeneration strategy, the molten salt approach follows the basic concept of thermal regeneration but uses Li salts that have a lower melting point than the temperature at which the reaction is run. As the Li source is effectively liquid, the main idea here is to practically solve the problem of having to calculate the correct amounts of Li salt for each sample, as well as the non-uniform distribution and crystallinity of the repaired LFP particles, as is the case in solid-state thermal regeneration [96,102,103,150]. Figure 7 shows a general flow scheme for this technique.

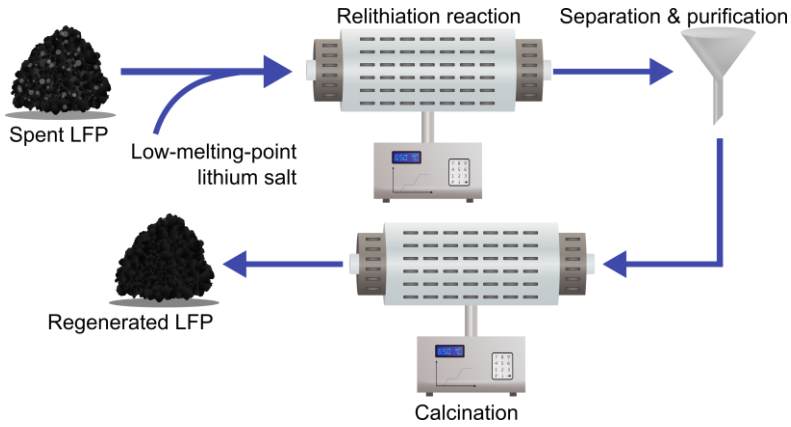

Figure 7. Illustration of the general molten salt-assisted regeneration technique.

This strategy is quite novel in the LFP field, and not much has been done yet. One example is the study by Liu et al., where spent LFP powders were mixed with excess lithium nitrate ($LiNO_3$), iron (II) oxalate (FeC_2O_4), and sucrose, and heated at 300 °C, i.e., some 50 °C above the melting point of $LiNO_3$, under Ar for different amounts of time. After quenching to room temperature, washing off the excess $LiNO_3$, and drying, the material was thermally treated in a solid-state fashion at 650 °C under Ar for 6 h. They found that there is an optimal time for the molten salt treatment at 2 h, below which the reaction is insufficient and above which the LFP particles tend to decompose into lithium phosphate (Li_3PO_4). Ultimately, clear improvements in electrochemical performance were made compared to the spent LFP batteries [104].

Wang et al. used the same salt and applied it to LFP black mass, rather than pure, carefully harvested LFP, as is the case in virtually all other direct recycling papers. The black mass was ball-milled with $LiNO_3$ and anhydrous glucose, and then heat-treated in air for 30 min at different temperatures. After quenching to room temperature and washing off the residual salt, the second annealing step was replaced with centrifuging in a saturated zinc chloride ($ZnCl_2$) solution for 5 min, thereby separating the regenerated LFP from the spent graphite. In agreement with Liu et al., the optimal temperature for the heat treatment was found to be 300 °C, yielding repaired CAM with a 97% improvement in rate performance, compared to the spent LFP, as well as a cycling stability over 500 cycles [149].

A dissolution recrystallization was done by Zhu et al., who employed a eutectic $LiNO_3$–LiOH mixture (3:2 mol) to create a liquid environment with higher dissolution capacity and high ion diffusion rates. The spent LFP, along with the eutectic salt mixture and citric acid (carbon source), were thermally treated at temperatures ranging from 350 °C to 550 °C

for 4 h, then washed with water, centrifuged, and dried. They achieved a competitive electrochemical performance for the regenerated CAM, with much better cycling stability than Liu et al., despite skipping the second heat treatment step [104,156].

3.3.3. Hydrothermal Regeneration

A more modern method, at least regarding LFP batteries, is the hydrothermal regeneration strategy. In fact, one of the first successful direct regeneration strategies was developed in 2004, using a hydrothermal method on spent LCO batteries [157]. Generally, hydrothermal regeneration comprises treatment of spent CAMs at elevated temperatures and pressures in a Li-containing aqueous solution, preferably also with a reducing agent to promote restoration of the original valence state of Fe [146]. Figure 8 shows an illustration of a general hydrothermal regeneration route.

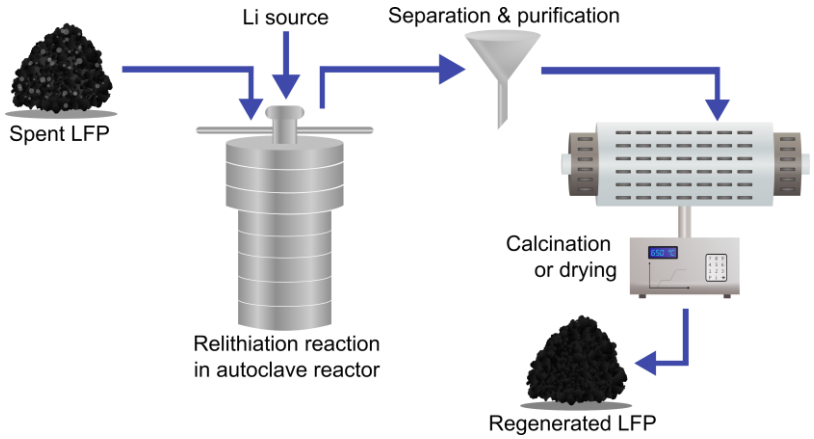

Figure 8. Illustration of a general hydrothermal regeneration technique.

The main advantage of the hydrothermal regeneration method is its much higher scalability compared to the thermal one. Specifically, it does not require exact amounts of Li source to be added to the reaction, since the unreacted Li salt can be reused for later operation [96,147]. It also offers vast improvements in terms of uniform distribution of Li, and thus also uniform crystallinity and morphology of the regenerated material, thereby ultimately putting more value into the regenerated CAM [96].

Probably the strongest argument against the hydrothermal strategy would be that there is a preference in the industry for a non-aqueous route, which is mainly related to the risk of HF formation upon contact between water and the possible electrolyte and/or binder residues. Also, the need for at least two heat treatment steps, as well as various chemicals, such as reducing agents, drives up the energy consumption of these methods [97,149]. Moreover, the high temperatures of the aqueous phases require high pressures, creating a need for expensive equipment [146,147].

In 2019, Song et al. demonstrated a hydrothermal regeneration of spent LFP electrodes by reacting them with LiOH, L-ascorbic acid (as a reducing agent), and sodium dodecylbenzene sulfonate ($C_{18}H_{29}SO_3Na$) at a series of temperatures (140–180 °C) and times (4–8 h). This was done after an initial pre-treatment involving calcination at 500 °C for 3 h to remove residues of binder and conductive carbon. For the regeneration reaction, to one of the samples, they even added graphene oxide regenerated directly from the spent batteries that were used as sources for the LFP electrodes. This was found to be beneficial, as this sample showed the best overall electrochemical performance in the subsequent tests, achieving a high discharge capacity of 163.3 mAh/g at 0.2 C and a previously unmatched cycling stability of 99.63% after 100 cycles at 0.2 C. The reaction conditions for this were 160 °C for 6 h with 5% graphene oxide added [158].

Tang et al. took a similar approach but skipped the initial high-temperature calcination of the spent powders, dissolving the binder in NMP instead. For hydrothermal regeneration, they mixed the spent LFP powders with a solution of LiOH and sodium sulfite (Na_2SO_3), heating the system in an autoclave reactor between 120 and 180 °C for 24 h, followed or not by Cu doping for improved performance by calcination with $Cu(NO_3)_2$ and glucose at 600 °C for 4 h in N_2. Interestingly, they also did a "traditional" solid-state thermal regeneration for comparison, by direct heat treatment with Li_2CO_3, glucose, and $Cu(NO_3)_2$ at 350 °C for 4 h and then at 650 °C for 12 h in N_2. Upon electrochemical testing, the hydrothermally regenerated samples showed better performance than the thermally regenerated ones, the best-performing one being regenerated at 150 °C followed by Cu doping (144 mAh/g at 0.1 C) [159].

To simplify the process further, Jing et al. regenerated spent LFP in a one-step reaction. The CAM, together with $Li_2SO_4{\cdot}H_2O$ and hydrazine ($N_2H_4{\cdot}H_2O$) as a reducing agent, was heated in an autoclave in a blast oven at 120–200 °C for 3 h. The only post-treatment was to wash the samples with deionized water and dry them at 80 °C for 10 h. With fewer steps, shorter treatment times, but slightly higher temperatures, they achieved better electrochemical performance than Tang et al., the best being recorded for the sample treated at 200 °C at 141.9 mAh/g at 1 C [150,159].

More recent research on the hydrothermal route was demonstrated by Jiang et al., who thought of implementing microwave irradiation on the reaction and developed a microwave hydrothermal (MWHT) relithiation strategy. LiOH and ascorbic acid were used for the regeneration, and the MWHT reaction was run at 120–180 °C for 1 h, or at 150 °C for different times. Like Song et al., Jiang et al. also regenerated the graphite from the spent anode sheets into graphene oxide employing a modified Hummers' method followed by microwave flash exfoliation, creating microwave-reduced graphene oxide (MWrGO). This was then used to dope the regenerated LFP (for performance improvement) by PDDA-assisted electrostatic self-assembly at different dopant concentrations for the MWHT reaction at 150 °C for 1 h, ultimately achieving electrochemical performance that was competitive to the one recorded by Song et al. [96,158].

Lacking cycling stability is a common obstacle for direct recyclers to overcome. Therefore, significant results were presented by Jia et al., who achieved a capacity retention of 80% over 1000 cycles at a current density as high as 10 C. This was done by raising the d-band center of Fe in the spent LFP, thereby strengthening the Fe–O bonds, effectively immobilizing the Fe and thus preventing the structural Fe_{Li} defects from forming during cycling. For this purpose, polyvinylpyrrolidone (PVP) was used as a source of N for the electron arrangement, forming N-doped carbon coated onto the LFP particles. In practice, this meant running a hydrothermal regeneration reaction with ethanol, lithium acetate (CH_3COOLi), and PVP at 180 °C for 5 h, followed by vacuum drying at 120 °C for 12 h and a subsequent sintering step at 700 °C for 5 h in Ar [97].

3.3.4. Chemical Regeneration

There is a natural strive in research and industry to lower the energy consumption of processes as much as possible. It is therefore of interest to explore possibilities to perform the direct regeneration of CAM in mild conditions, such as at ambient temperatures and pressures. This becomes especially interesting when addressing LFP and other less expensive CAMs, where the economic incentive for recycling is intrinsically low. What we refer to as the chemical regeneration route comprises the treatment of spent LFP powders in an aqueous or organic solution at mild or quasi-mild conditions, i.e., temperatures and pressures at ambient or only slightly elevated levels [146]. Figure 9 shows an illustration of a general chemical regeneration route.

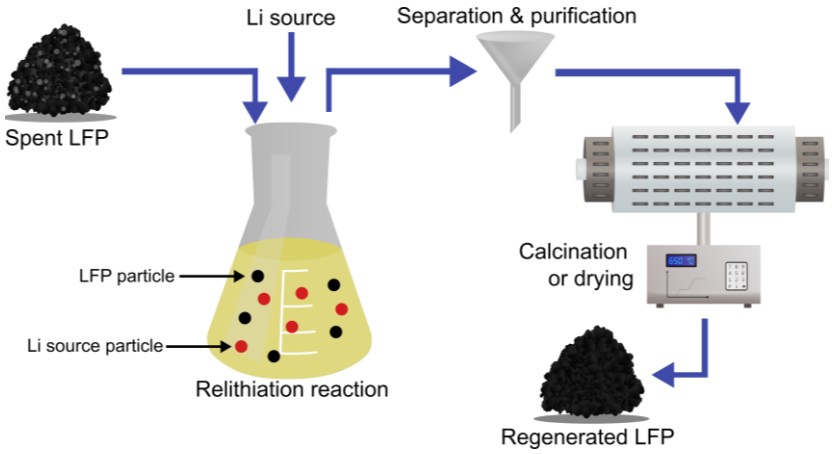

Figure 9. Illustration of a general chemical regeneration technique.

Besides the low energy consumption of the chemical methods, other advantages are their simplicity, possibly good atom economy, great potential for scalability, and usability for different electrode degradation states or even different electrode types [146,160]. On the contrary, full recovery of the crystal structure of the CAM seems to be problematic at present, implying a need for consecutive heat treatment. Moreover, if organic solvents are used, there is a risk of secondary air pollution from these processes [147].

The first overall paper on direct regeneration of LFP to our knowledge is the one by Ganter et al. (2014), where both a chemical and an electrochemical were used and compared. For the chemical relithiation, the spent LFP was put into a lithium iodide (LiI) solution in acetonitrile and stirred for 20 h, and then filtered and vacuum-dried at 100 °C for 1 h, recording a specific capacity close to the one reported for a new commercial cathode, i.e., 153 mAh/g at 0.1 C [161]. Ouaneche et al. tried the same approach but compared several different solvents, including acetonitrile, ethanol, methanol, cyclohexane, DMSO, and propylene glycol. Fortunately, for the economical aspect of a possible upscaling of the method, the best electrochemical performance, as much as 160 mAh/g discharge capacity at 1 C, was recorded for the sample regenerated in ethanol, which is one of the cheapest organic solvents [162]. Another organic regeneration strategy is from Wu et al., who employed lithiated organic reagents including pyrene ($C_{16}H_{10}$), biphenyl ($C_{12}H_{10}$), naphthalene ($C_{10}H_8$), and perylene ($C_{20}H_{12}$) for regeneration of spent cathodes of different types. This was done by simple stirring for 15 min, followed by centrifugation and air drying at 80 °C. For LFP, the best results were obtained after relithiation with the lithiated pyrene reagent, restoring its capacity to the level of commercial LFP (155 mAh/g at 0.5 C) [160].

To lower the risk of secondary pollution from organic solutions, as well as the price of the proposed methods, chemical relithiation can also be performed in aqueous solutions. Xu et al. used LiOH and citric acid as a reducing agent in solution while heating at a range of temperatures between 60 and 180 °C for various reaction times, thereby touching hydrothermal regeneration. This was followed by a thermal annealing step with Li_2CO_3 for 2 h under N_2. They found that lowering the temperature to 80 °C did not influence the reaction kinetics significantly. Also, by slightly extending the reaction time to 10 and 17 h, respectively, one could reduce the temperature to as low as 70 or 60 °C, respectively, allowing regeneration at ambient pressure. Hence, this work is placed in the chemical regeneration category. The resulting electrode exhibited cycling stability over as much as 1000 cycles [111]. Xu et al. employed a similar strategy, exchanging citric acid for H_2O_2 and lowering the reaction temperatures to as low as 10–50 °C with reaction times between 10 min and 5 h, achieving cycling stabilities similar to those in a previous study [111,163]. Focusing on the use of LiOH for aqueous solution regeneration, Sun et al. developed a

two-step "ice & fire" method, using glucose as a reducing agent and carbon source, with NaCl as a templating agent to embed in the glucose and form 3D-interconnected porous carbon networks on the LFP particles for better performance. The solution was heated at 60 °C for 2 h under stirring, before going through freeze drying in vacuum along with added urea for N doping of the carbon coating for further improvement in performance. Finally, a heat treatment step at 650 °C for 3 h in Ar was performed, ultimately achieving electrochemical performance with high discharge capacities and retention rates [102].

Im et al. obtained recycled Li_3PO_4 cleverly refined from the wastewater of an existing LIB treatment plant. It was used as a precursor to synthesize $LiFePO_4$ by mixing with $Fe(NO_3)_3$, phosphoric acid, and citric acid in a triethylene glycol–water blend, followed by spray pyrolysis and subsequent sintering at 800 °C in N_2, reaching a comparable performance of 161 mAh/g [164].

In the most recent research on chemical regeneration, Song et al. used ultrasonication at ambient conditions to create local shock waves with high temperature and pressure in the material, thus creating a quasi-hydrothermal regeneration environment without the need for expensive heat treatment in an autoclave reactor. The solution was a mixture of lithium chloride (LiCl) with hydrazine hydrate ($N_2H_4 \cdot H_2O$) as a reducing agent in a 50/50 blend of ethylene glycol and water. After sonication for 25 + 25 min with a 10 min break in between, and subsequent centrifugation and washing steps, the regenerated material with 1 M LiCl and 1.5 mL $N_2H_4 \cdot H_2O$ exhibited the best performance, with a slightly lower discharge capacity but high retention rate at 97% after 100 cycles at 1 C [109].

3.3.5. Electrochemical Regeneration

Unlike its competitors, this technique relies on electrochemical force to relithiate the CAM by electric cycling, rather than by some chemical or physical treatment. The main advantage is the mild conditions, facilitating relatively low energy consumption, reduced usage of chemicals, and minimal secondary pollution and waste generation [146]. However, this method relies on simply providing active lithium to the spent CAM materials without further treatments to help repair the damaged crystalline structure. Research on this technique thus struggles to match the electrochemical performance of LFP repaired by other means [147]. Also, if expensive lithium foil is used as the counter-electrode for the cycling operation, the economic incentives for this method suffer. This technique is illustrated in a general form in Figure 10.

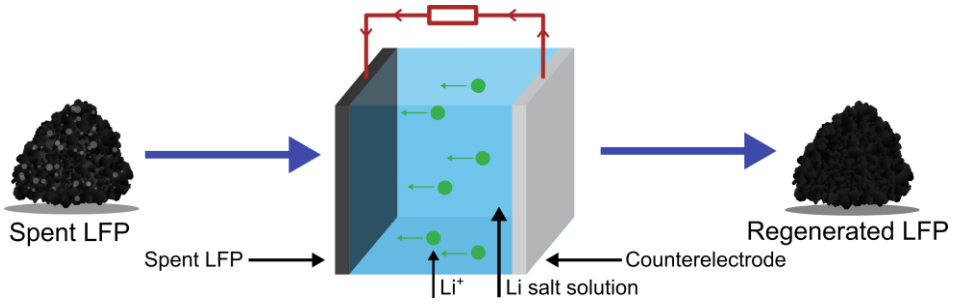

Figure 10. Illustration of a general electrochemical regeneration technique.

As previously mentioned, the first to demonstrate the electrochemical regeneration of LFP were Ganter et al., in 2014. Here, the spent LFP was cycled with lithium multiple times, and then fully discharged, lithiated, and assembled with a capacity-matched fresh negative electrode. They achieved complete restoration of the initial discharge capacity compared to a fresh electrode, but with lower capacity retention [161].

Later, Wang et al. suggested a different, very simplistic approach to the relithiation of spent LFP by pairing it with a prelithiated graphite anode without any particular treatment of the spent cathode, reaching modest electrochemical performance at best [165]. Li et al. managed to achieve improvements in terms of cycling stability by developing the method into an external short-circuit technique, where spent positive electrodes were paired with lithiated materials consisting of lithiated graphite (LiC_6) and metallic lithium. The electrochemical cells created this way, with a standard $LiPF_6$ electrolyte and polypropylene separator, were then wrapped in aluminum foil and the reaction was left to take place spontaneously, consuming no external energy. After cleaning with dimethyl carbonate (DMC) and vacuum drying, the regenerated LFP electrodes were directly obtained [166]. Recently, Fan et al. achieved further improvements in the performance of regenerated cathodes by using a functionalized prelithiated separator instead of a prelithiated anode. A spent LFP cathode was paired with a fresh graphite anode and assembled with a prelithiated separator, prepared by coating a layer of a lithium oxalate ($Li_2C_2O_4$)–CMK-3 (ordered mesoporous carbon) composite on it, followed by cycling the as-prepared cell once at 0.05 C between 2.5 and 4.5 V at ambient temperature [167].

3.4. The Indirect Approach

Despite having been on the market for a decade and having demonstrated the feasibility of regenerating degraded LIB CAMs, the direct regeneration strategies described above struggle to get much industrial attention. Most importantly, the lack of standardization of the manufactured batteries in terms of sizes and measures causes batteries from different manufacturers to look different. At present, this renders industrial automation of direct recycling processes difficult, as the positive electrodes need to be harvested as clean as possible, preferably individually and with little to no impurities, for the regeneration process to be successful. Therefore, research has been focusing on the regeneration of manually harvested cathodes from manually discharged and disassembled batteries. This poses obvious challenges for industrial applications, such as the lack of incentive from recyclers to let staff dismantle large volumes of batteries by hand, rather than simply smelting or grinding them in automated processes. However, for batteries with intrinsically low added value, such as LFP batteries, this may prove to be the only viable option, given the high operational costs of pyro- and hydrometallurgy, as well as the relatively low value of the products obtained from these batteries. This is, of course, unless the regeneration strategies can be applied directly to the black mass coming from shredding of the spent batteries and subsequent material separations, turning "regeneration" into "resynthesis". This hybrid approach is what we like to call the "indirect direct recycling", or the indirect approach. Although the reported techniques are quite different, Figure 11 shows a generalized flow scheme of the indirect route.

Apart from the already mentioned advantage of the "indirect" approach, it is worth noting that research done in this way generally reports higher capacity retention rates for the resynthesized CAM—something that increases their added value. On the other hand, the route through crushing and hydrometallurgical treatment of the spent batteries before electrode resynthesis inevitably adds steps and complexity to the processes, ultimately driving up the operational and investment costs. If, however, the revenue for selling resynthesized positive electrodes with pristine-level performances is much higher than that of the hydrometallurgical products, then such a process may turn out to be a viable option if fine-tuned for an existing LIB treatment process that already produces the black mass.

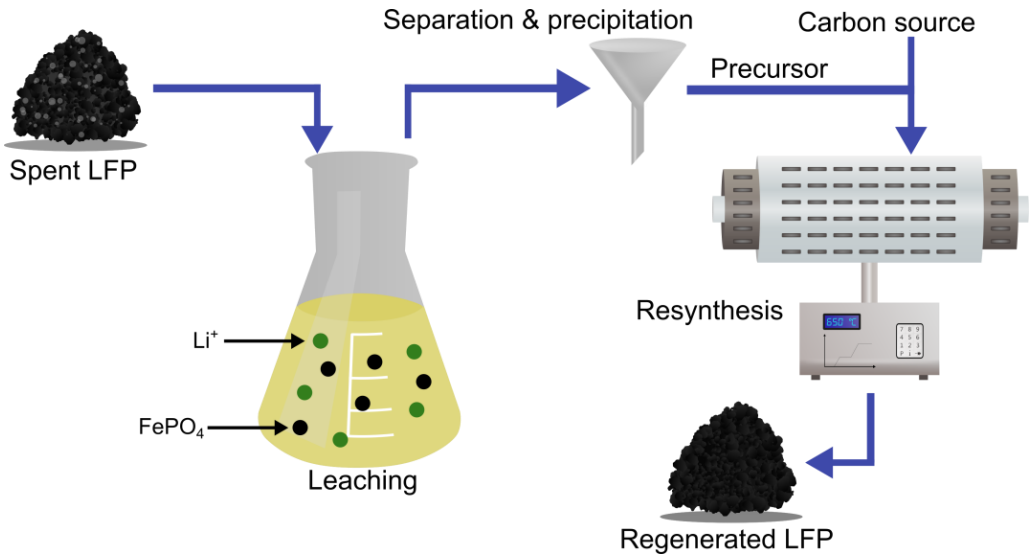

Figure 11. Illustration of a general indirect recycling route.

To the best of our knowledge, the first to present a working process for a spent LFP resynthesis route were Shin et al., in 2015. They started with thermal annealing at 700 °C and then leached the spent cathode powders with HCl with subsequent pH adjustment with ammonium hydroxide (NH_3OH) to precipitate amorphous $FePO_4 \cdot xH_2O$ and crystalline $FePO_4 \cdot 2H_2O$. The crystalline $FePO_4$ was then calcined with LiOH and sucrose at 700 °C in Ar/H_2, and the specific capacity (SC) obtained was 139 mAh/g [168]. Wang et al. employed a similar strategy up to the $FePO_4$ precipitation. They, however, continued the pH adjustment up to 7, accompanied by the addition of Na_3PO_4, precipitating Li_3PO_4. This was then purified and used as a precursor, along with $FeSO_4 \cdot 7H_2O$ and ascorbic acid, to prepare $LiFePO_4$ using a hydrothermal method followed by solid-state sintering at 600 °C with added glucose, achieving an improvement in SC of 144 mAh/g [103].

In recent years, researchers seem to widely focus on recovering one specific precursor material from the spent LFP batteries, i.e., Li_2CO_3, which is then used for the synthesis of new LFP by some variation of the thermal method. Instead of finding new precursors to recover, focus seems to have shifted towards employing milder reaction conditions to save energy, equipment, and environment. In particular, the use of organic acids and reducing agents has gained some attention. Kumar et al. leached a spent LFP electrode with different citric fruit juices accompanied by H_2O_2 as a reducing agent. After recovering $FePO_4$ and Li_2CO_3, the precursors, along with added glucose, were calcined at 700 °C in Ar, reaching satisfactory electrochemical performance, of 155 mAh/g at 0.1 C, for the use of such complex and unpurified reagents as fruit juices [52].

A similar approach, but without an organic acid, was used by Kong et al., who performed oxidation leaching with sodium hypochlorite and HCl for pH regulation. After precipitation of $FePO_4$ and Li_2CO_3, the refined precursors along with added sucrose were used to synthesize LFP by heat treatment at 350 °C and 750 °C, reaching an SC of 154 mAh/g [117]. Sulfuric acid has been widely used for leaching, and the highest specific capacity (160 mAh/g) in a resynthesized LFP was obtained by Fu et al. Using 2.5 M H_2SO_4 and H_2O_2 for oxidation, the positive electrode was resynthesized with recovered Li_2CO_3 and $FePO_4$ and glucose at 700 °C. Such good results were obtained due to precise pH adjustment during the precipitation step, where Al and Cu impurities were removed, and iron was completely separated from lithium ion [169]. Oxidation leaching was also employed by Peng et al. with ammonium persulfate ($(NH_4)_2S_2O_8$) and separating the $FePO_4$ phase from the Al foil only after the leaching. The recovered Li_2CO_3, $FePO_4$, and

added glucose were then sintered at 750 °C to obtain the resynthesized LFP, achieving at the highest 148 mAh/g and high capacity retention of 98% after 400 cycles at 1 C [170]. Similarly, Sun et al. employed oxidation leaching with $(NH_4)_2S_2O_8$, while precipitating first the Fe by NaOH and then the Li_2CO_3 with Na_2CO_3 at an elevated temperature of 95 °C. After refining the Fe into $FePO_4$ by calcination at 700 °C in O_2, the usual calcination with added glucose was performed at 350 °C and 700 °C in N_2, reaching an improvement in the discharge capacities (156 mAh/g) compared with Peng et al. [171].

Xu et al. used the oxidative leaching strategy with H_2O_2 directly on whole spent cathode sheets without prior separation from the current collector foil. Instead, the $FePO_4$ and Al foil left in the leaching residue were separated easily after vacuum drying, and the recovered $FePO_4$ was used as a precursor for the preparation of new LFP. This was done by annealing with LiOH and glucose at 350 °C and 650 °C in Ar, achieving an SC of 137 mAh/g [172]. Conversely, Hu et al. employed acid leaching with H_3PO_4 and citric acid and argued for a pre-removal of the Al, as they found that fewer Al impurities in the regenerated LFP yielded notably better performance (145 mAh/g), especially in terms of cycling stability of 97% retention for 600 cycles. This was done by simply adding a diluted LiOH solution to the leaching system. Then, Li_2O_3 and Li_2CO_3 were used to adjust the molar ratios in the leaching environment, along with the addition of starch as a carbon source. After a sanding process and spray drying, the LFP/C precursor was sintered at 450 °C and 700 °C in Ar [173].

An innovative approach was recently employed by Wang et al., where both the elemental extraction and the subsequent resynthesis of LFP were performed in a “one pot” manner. More specifically, Li was extracted by leaching with citric acid and H_2O_2 in a zirconia bead ball mill, after which the recovered precursors ($FePO_4$, LiOH, and Li_3Cit) were directly calcined in the traditional way at 350 °C and 650 °C in Ar, ultimately reaching 102 mAh/g with 90% retention in a cycling stability of 1000 [174].

Table 2. Overview of direct recycling strategies and the corresponding best-recorded electrochemical performance of the regenerated positive electrodes. * = value obtained from figure, DI = deionized water, n/r = not reported, FP = $FePO_4$.

Method	Conditions	Electrochemical Performance					Ref.
		Discharge Capacity [mAh g^{-1}]	At Current Density [C]	Capacity Retention [%]	After Cycles	At Current Density [C]	
Thermal (solid-state)	Thermal annealing under Ar/H_2 at 600 °C for 1 h	132	1	n/r	n/r	n/r	[151]
	Pristine LFP doping at different ratios, sintering at 700 °C for 8 h under N_2	144	0.1	93.75	100	0.2	[112]
	Thermal annealing under Ar/H_2 at 650 °C for 1 h w/Li_2CO_3	147.3	0.2	95	100	0.2	[152]
	NaOH wash, annealing at 450 °C for 2 h under air, added Li/Fe/P salts, ball mill, spray drying, annealing at 650 °C for 10 h under N_2	139	0.2	95	100	0.2	[153]
	Li_2CO_3 + glucose, annealing at 350 °C for 4 h, then 650 °C for 9 h	161.1	0.1	91	200	1	[107]
	Li_2CO_3 + glucose in DI, thermal annealing at 350–900 °C, ball mill, grinding, calcination	148	0.05	92.9	100	0.1	[99]
	Calcination at 550 °C for 2 h under air, sieving, Li_2CO_3 + glucose, ball mill, drying at 60 °C for 12 h, annealing at 700 °C for 8/10/12 h under N_2 w/TiO_2 doping	147.3	0.1	94.1	100	0.5	[154]
	Li_2DHBN, grinding, sintering at 800 °C for 6 h under Ar/H_2	127	2	88	400	5	[155]
	Li_2CO_3 + glucose + CNT, ball mill in EtOH:H_2O 1:1, drying at 80 °C, annealing at 350 °C for 2 h, then 650 °C for 12 h under Ar	155.15	0.05	93.8	100	0.1	[109]
	Li_2CO_3 + glucose + $Cu(NO_3)_2 \cdot 2.5H_2O$, ball mill in EtOH, drying, annealing at 350 °C for 2 h, then 650 °C for 12 h under Ar	160.15	0.05	81.19	1000	1	[108]
Molten salt	$LiNO_3$:LiOH 3:2 + citric acid, heating at 350/450/550 °C for 4 h, DI wash, centrifuge, drying at 80 °C for 12 h	151.2	0.2	97.73	150	1	[156]
	$LiNO_3$ + FeC_2O_4 + sucrose, heating at 300 °C for 1–6 h under Ar, room temp. quench, DI wash, centrifugation, drying at 80 °C for 12 h, annealing at 650 °C for 6 h under Ar	145	0.5	90	100	0.5	[104]
	$LiNO_3$ + anhydrous glucose, ball mill, annealing at different temps., room temp. quench (DI), DI and EtOH wash, centrifuge in $ZnCl_2$(aq), DI wash	162	0.1	90	500	0.1	[149]

Table 2. *Cont.*

Method	Conditions	Electrochemical Performance					Ref.
		Discharge Capacity [mAh g^{-1}]	At Current Density [C]	Capacity Retention [%]	After Cycles	At Current Density [C]	
Hydrothermal	$Li_2SO_4 \cdot H_2O$ + hydrazine, autoclave, magnetic stirring for 10 min, blast oven for 3 h, filtering and DI wash, drying at 80 °C for 10 h	141.9	1	98.6	200	1	[150]
	LiOH + Na_2SO_3 in autoclave, heating at 150 °C for 24 h, cooling, doping w/$Cu(NO_3)_2$, calcination at 600 °C for 4 h under N_2	144.02	0.1	92.36	100	0.2	[159]
	LiOH + ascorbic acid in DI, microwave hydrothermal reduction, graphene doping, MWHT reduction, wash and filter	161.4	0.2	94.9	100	0.2	[96]
	PVP + S-LFP in autoclave w/EtOH, added CH_3COOLi, heating at 180 °C for 5 h, centrifuge, vacuum drying at 120 °C for 12 h, sintering at 700 °C for 5 h under Ar	139.1	1	80	1000	10	[97]
	LiOH + ascorbic acid + SDBS in DI, hydrothermal heating, regenerated GO added (5%) to 160 °C for 6 h regeneration	163.3	0.2	99.63	100	0.2	[158]
Chemical	LiI in EtOH mixed w/SLFP, filtration, washing w/EtOH, drying at 100 °C for 1 h under vacuum, grinding	160	1	n/r	n/r	n/r	[162]
	LiOH + citric acid, range of T and time, DI rinse, thermal annealing w/Li_2CO_3 for 2 h under N_2	159	0.5	94.34	1000	0.5	[111]
	Pristine LFP, chemical oxidation, degraded LFP, + polycyclic aryl-Li compounds, stirring, centrifugation, drying at 80 °C in air overnight	155 *	0.5	97 *	100	0.5	[160]
	LiI in acetonitrile, stirring for 20 h, vacuum filtration, rinse w/acetonitrile, drying at 100 °C for 1 h under vacuum, grinding	153 *	0.1	n/r	n/r	n/r	[161]
	LiOH + glucose + NaCl into DI, stirring at 60 °C for 2 h, freeze drying (vacuum) overnight w/urea, heating at 650 °C for 3 h under Ar, cooling, DI rinse, vacuum drying	169.74	0.1	95.7	200	0.1	[102]
	LiCl + $N_2H_4xH_2O$ in 50% ethylene glycol/water solution, ultrasonication for 25 min—10 min rest—25 min again, centrifuge, DI and EtOH wash	135.1	1	97.44	100	1	[109]

Table 2. *Cont.*

Method	Conditions	Electrochemical Performance					Ref.
		Discharge Capacity [mAh g^{-1}]	At Current Density [C]	Capacity Retention [%]	After Cycles	At Current Density [C]	
Chemical	$LiOH + H_2O_2$ in solution, DI rinse to remove LiOH residues, vacuum drying, thermal annealing w/Li_2CO_3 under Ar at 400–800 °C for 2–10 h	146.3	1	84.9	1000	5	[163]
	Li_3PO_4 from wastewater + DI, mixed w/$Fe(NO_3)_3$ + phosphoric + citric acid in DI and TEG, spray pyrolysis, room T cooling, sintering at 800 °C for 2 h under N_2	161.3	0.1	99.87	50	0.1	[164]
Electrochemical	Lithiated graphite, cell assembly w/S-LFP wrapped in Al foil, time-controlled regeneration, cleaning w/DMC => drying for 4 h under vacuum	125.4	0.5	98.8	100	0.5	[166]
	Cycling w/Li(s), discharge to lithiate positive electrode, coin cell assembly, pairing w/fresh negative electrode	140 *	0.1	81 *	50	0.1	[161]
	Cycling, washing w/DMC, positive electrode separation, pouch cell assembly w/prelithiated graphite as negative electrode, cycling	126.6	0.5	62.5	200	0.5	[165]
	Cycling, LFP coupled w/fresh graphite + functionalized prelithiation separator, 1 cycle at <0.05 C	158.4	0.5	90.7	292	0.05	[167]

Table 3. Overview of the direct recycling using the "indirect" route and the reported electrochemical performance of the regenerated LFP positive electrode materials. The precursors to re-synthesized LFP are the recovered Li_2CO_3, $FePO_4$; otherwise, they are mentioned. Specific capacity (SC) and its retention after a certain number of cycles refer to the same current density (1 C); otherwise, it is mentioned. * = value obtained from figure, n/r = not reported.

Leaching Agent	Conditions	Leaching Efficiency [%]				Electrochemical Performance of Resynthesized LFP		Ref.
		Li	Fe	P	Others	Discharge Capacity [mAh g^{-1}]	Retention [%] (#Cycles)	
H_2SO_4	2.5 M H_2SO_4, L/S = 10 mL/g, 60 °C, 4 h. Less than 0.005% of impurities.	97	98		S < 0.018	137.8	n/r	[138]
	9 M H_2SO_4, L/S = 10 mL/g, air oxygen as oxidant, air flow rate = 60 mL/min, 25 °C, 5 h. No impurities.	99.3	0.02	0.02		131.7	99 (100)	[55]
	H_2SO_4 = 1.5 times the theoretical amount, L/S = 4 mL/g, ascorbic acid (3%wt) as reducing agent to prevent the formation of Fe^{3+}, 60 °C, 4 h. Purity > 98%.	98	98	98		133	~100 (100)	[175]
	2 M H_2SO_4, L/S = 20:1, 70 °C, 2 h. No impurities. Filtrate Li^+, added $FeSO_4$, H_3PO_4, LiOH.	96.67	93.25	n/r		105	98.6 (300)	[176]
	2 M H_2SO_4 and H_2O_2, S/L = 30 g/L, H_2SO_4/H_2O_2 = 4 *v*/*v*, 60 °C, 80 min. No impurities. Fe_2O_3 added Li_2CO_3.	n/r	n/r	n/r		141	95 (100)	[177]
	2.5 M H_2SO_4 and H_2O_2 (30%mass), L/S = 25 mL/g, 60 °C, 1 h. No impurities.	98.79	94.97	98.71		160.1 (0.1 C)	99.7 (100)	[169]
HCl	LFP powder pre-treated at 700 °C, 10 h, to decompose carbon and oxidize Fe^{2+} to Fe^{3+}. Leaching: 6 M HCl, 120 °C, 6 h. Recovered: $LiOH.H_2O$.	n/r	n/r	n/r		139.03	98.95 (25)	[168]
	LFP powder pre-treated at 600 °C, to oxidize iron. Leaching: 4 M HCl. Recovered: Li_3PO_4.	n/r	n/r	n/r		144.3	96.7 (200)	[103]
H_3PO_4	0.5 M H_3PO_4, 25 °C, 1 h. $FePO_4 \cdot 2H_2O$ was precipitated with reflux for 9 h at 85 °C. Recovered: $FePO_4 \cdot 2H_2O$.	n/r	n/r	n/r		110 (5 C)	95.4 (100)	[178]
	2.3 M H_3PO_4 and 0.58 M citric acid, L/S = 5:1, 50 °C, 3 h.	95.1	96.2	n/r	Al	145.4	97.3 (600)	[173]

Table 3. *Cont.*

Leaching Agent	Conditions	Leaching Efficiency [%]				Electrochemical Performance of Resynthesized LFP		Ref.
		Li	Fe	P	Others	Discharge Capacity [mAh g^{-1}]	Retention [%] (#Cycles)	
Citric acid	Lemon juice and H_2O_2 (6%vol), S/L = 67 g/L, 25 °C, 90 min.	94.83	4.05	0.84	Cu = 96.9 Al = 47.2	135.3	98.3 (100)	[52]
	$C_6H_8O_7$ and 2 mL H_2O_2 (30%) in ball mill with zirconia beads, 200 rpm, 30 min. Recovered: LiOH, Li_3Cit.	98.21	<1.5	n/r		102.5 (5 C)	90 (1000)	[174]
	0.25 M $C_6H_8O_7$, 40 °C, 2 h, (i) without and (ii) with H_2O_2 (6%vol). (iii) Comparing the leaching with 1 M H_2SO_4, 25 °C, 1 h.	(i) = 90 (ii) = 87 (iii) = 95	(i) = 99 (iii) = 98	(i) = 69 (iii) = 96	S, Al, Cl, Co, V	n/r	n/r	[98]
Acetic acid	0.8 M CH_3COOH and H_2O_2 (6%vol), S/L = 120 g/L, 50 °C, 30 min.	95.13	n/r	n/r		130 * (0.1 C)	n/r	[143]
Pyrophosphoric acid	9 M $H_4P_2O_7$, oxygen as oxidant, S/L = 100 g/L, oxygen flow = 20 L/min, 25 °C, 5 h.	97.98	~100	n/r		150.2	91.31 (100)	[179]
Sodium hypochlorite	NaClO (12% available Cl), S/L = 50 g/L, 30 °C, 2 h.	98.3	0.11	n/r	Al ~0	154.3	92.7 (300)	[117]
Iron salt	80 mM $FeSO_4 \cdot 7H_2O$ and 400 mM H_2O_2 (30%vol), slurry density = 20 g/L, 40 °C, 30 min.	99.9	n/r	n/r		138.9 (0.5 C)	93.6 (50)	[180]
Organic solvent	4 M methanesulfonic acid (MSA), S/L = 80 g/L; 4 M p-toluenesulfonic acid (TsOH), S/L = 60 g/L. Both with H_2O_2 (18%vol), 25 °C, 90 min.	MSA = 96 TsOH = 97	99	n/r	MSA: Cu, Al TsOH: Cu	80	n/r	[181]
H_2O_2	H_2O_2 (20%vol), S/L = 15 g/L, 40 °C, 20 min.	96.3	n/r	n/r		137.1	97.9 * (250)	[172]
Ammonium persulfate	$(NH_4)_2S_2O_8$ = 1.4 times the theoretical amount, S/L = 50 g/L, 30 °C, 30 min.	98.1	0.02	n/r	Al = 0.06	130.2	98 (400)	[170]
	LFP and $(NH_4)_2S_2O_8$ in water for 30 min.	34.3	1.31	2.03		145.2	97.9 (200)	[182]
	$(NH_4)_2S_2O_8$ = 1.3 times the theoretical amount, S/L = 150 g/L, 25 °C, 1 h.	52.4	n/r	n/r		156.1 (0.2 C)	98.4 (100)	[171]

4. Perspectives and Challenges with Direct Recycling

As can be seen, a lot of research has been done on the direct recycling of LFP battery positive electrodes. Overall, all methods have their advantages and disadvantages, as summarized in Table 4.

Table 4. Summary of the advantages and disadvantages of the different direct recycling methods, as well as the indirect approach.

Method	Advantages	Disadvantages
Thermal (solid-state)	• Simple • Few steps • Minimized chemical consumption	• Secondary pollution by toxic gas exhaust • Non-uniform Li distribution • Non-uniform crystallinity and morphology • Low scalability
Molten salt	• Simple • Few steps • Higher scalability • Uniform Li distribution • Uniform crystallinity and morphology	• Low technology readiness • $LiNO_3$ is oxidative—need for an extra reducing agent • Still needs thermal treatment
Hydrothermal	• High scalability • Uniform Li distribution • Uniform crystallinity and morphology	• Industrial drive towards dry methods • Risk of HF formation • High chemical consumption • Still needs thermal treatment
Chemical	• Mild conditions—green chemistry • Low energy consumption • Simple • Potential high atom economy • Scalability and applicability	• Performance issues for the regenerated CAM—heat treatment may be needed • High chemical consumption • Possibly toxic reagents needed—risk for secondary pollution
Electrochemical	• Mild conditions • Low energy consumption • Reduced chemical usage • Minimal secondary pollution • Minimal waste generation	• Relies on providing a source of active Li^+, such as metallic Li or fresh LFP • Low economic incentive • Performance issues for the regenerated materials
Indirect	• Fits existing LIB treatment infrastructure • Possibly applicable to the black mass directly • High performance of products	• Many steps • Higher complexity of the processes • High operational costs

Since none of them has really made it into a real industrial application, it is difficult to determine which factor is the most important in the transition from a lab-scale technique to an industrial practice. In fact, there are a couple of dilemmas to be solved before we can expect to see these techniques being upscaled. First, there is the question of safety. LIBs can induce (often justified) fear when handled, owing to their toxic and flammable, sometimes even explosive, nature. What is more, manual disassembly of the amounts

of discarded batteries that will need to be recycled would be an economically infeasible process for industries to invest in, no matter how well the final product performs. Not only would this take too much time, but workers being potentially exposed to electrolyte fumes daily would surely become a work environment issue. In combination with the previously discussed lack of standardization of the batteries, this means that a direct recycling process should either be versatile/smart enough to be automated in at least a few different battery types/dimensions with automated manual disassembly or be simple enough so that every battery manufacturer can build a small recycling facility, where the process would be adjusted to their specific products. The alternative would be a process that simply omits the manual disassembly and works with whatever an existing LIB treatment process can offer, i.e., the indirect approach. What will eventually be implemented by the industry and at what form/scale is difficult to predict.

Table 2 presents a quantitative comparison of all the previously mentioned direct recycling research in terms of the quality of the end product. More specifically, the best (or most comparable) recorded results from each paper are shown, along with a brief description of the applied method. By results, we mean the electrochemical performance of the regenerated/resynthesized electrodes when tested, where the discharge capacity at a specified current density is presented alongside the capacity retention after a certain number of cycles at a certain current density. What can be seen is a wide distribution of reported performance and the ways in which it is reported. Generally, the performance tends to improve as the research progresses, but upon reading deeper into the publications, it becomes clear that there is still a lot to be understood about the interactions inside and outside of the battery materials. Many times, in fact, researchers do not seem to agree on some basic questions, such as whether it is enough to supplement the lost active lithium without further thermal treatment for the CAM to be considered regenerated. It is safe to say that the technology readiness level of these techniques is still low, and despite the extensive research, there is still a lot to be explained and solved before an industrial application is in its place, all while the need for an efficient and feasible LFP recycling method becomes more and more pressing.

When the LFP electrode is resynthesized through the indirect method, most of the reported work has a leaching efficiency for lithium greater than 90%, and in many cases, the leaching efficiency for lithium is greater than 98% (Table 3). These values are important in complying with Regulation (EU) 2023/1542 of the European Parliament and of the Council of 12 July 2023 concerning batteries and waste batteries, which determines that by the year 2032, recycling processes must recover 80% of lithium. Generally, the final products are Li_2CO_3 and $FePO_4$, and high purity is reported. Most cases of LFP resynthesis reported a specific capacity greater than 130 mAh/g at 1 C after 100 cycles, with capacity retention averaging 95% (Table 3). This value is within the range of a new commercial LFP electrode, which is 120 to 160 mAh/g [51,183–185]. Values close to the upper limit of SC can be obtained when there is good separation of lithium and iron in the hydrometallurgical process, as well as reduced amounts of impurities, such as aluminum and copper.

There is also the question of the efficiency and effectiveness of the proposed methods. In most cases, iron is obtained as $FePO_4$ and lithium is precipitated as Li_2CO_3 using Na_2CO_3; however, there is no description of how much sodium salt ($NaSO_4$ when sulfuric acid is used as leaching agent, for example) is produced as a by-product in the precipitation step. Furthermore, there is no description of the generation of effluents and their treatment or disposal, such as the water used to wash the solid in the filtration step.

Future Outlooks

Given the growing stock of LIB waste and its content of critical raw materials, as well as the upcoming EU-wide regulations, we can expect to see recycling efforts emerge in the industrial sector. Even if the technology may not be fully ready yet, producers and recyclers will be forced to act and will likely pick a technology to invest in. The three most important factors in the choice making will probably be the cost of the technology, its simplicity and versatility, and the quality of the end product. Despite its complexity, we believe that the indirect approach will likely become the first choice of recyclers, mostly owing to its ability to integrate with existing recycling outputs, i.e., the black mass.

Other techniques will probably be developed further until one technique satisfies the criteria of industrial shareholders and becomes an attractive investment. So far, the solid-state regeneration strategy has the highest potential for this, since it is the most understood technique that is, in fact, used for the synthesis of fresh LFP. It is also relatively simple and capable of producing well-performing regenerated LFP. The need for precise quantification of lithium loss is still a challenge that needs to be overcome. Perhaps the upcoming mandatory battery passports will contain enough information about a battery to provide a rough estimate of its degradation state. Also, if automation and spectroscopy technologies continue to be improved in other fields of research, dismantling and precise characterization of discarded batteries will become less of a challenge in the future.

Considering the future of the entire battery market, it is important to realize that the batteries themselves are continuously being developed. Given the status of lithium as a critical raw material, the acquisition of which is challenged by concerns for environmental pollution and human health, as well as a changing geopolitical climate, we expect the development of new battery technologies to shift away from lithium-based electrodes and towards more accessible materials, such as sodium. The development of Na-ion batteries is, indeed, ongoing [186–189], and if successful, these batteries could eventually replace Li-ion batteries altogether. Then, new recycling technologies will have to be developed.

5. Conclusions

High recovery of LFP battery elements is achieved through hydrometallurgy, and direct positive electrode recycling is developing with promising industrial feasibility. It is expected that a circular economy can be created for LFP batteries, enabling the recycling of the positive and negative electrode and the electrolyte. To achieve this, the final product from recycling must be of good quality, with low levels of impurities, so that it can be used in the manufacture of new batteries. In the case of direct CAM regeneration, the resulting electrochemical performance is of great importance, as it will determine the incentive to develop methods for industrial applications. The direct thermal method is the most studied, and, on average, specific capacities above 140 mAh/g are reported. This method is improved by reducing the working temperature by molten salt, with an SC of around 150 mAh/g. This route is promising for industrial applications and needs further development. The “indirect” direct recycling, in which CAM is re-synthesized after leaching of the elements, is extensively studied, and the reported SC results are above 130 mAh/g. However, clarification is needed regarding the secondary products and effluents that are formed, such as $NaSO_4$ formed when pH is changed, and the water used for washing the precipitated solid. Given the extensive research efforts and the state of industrial recycling of LFP, it is clear that the ultimate recycling strategy is yet to be found and that the development needs to continue. Despite achieving high discharge capacities and capacity retentions, recycling methods also need to address issues such as technical complexity, techno-economic feasibility, and safety. Therefore, more research in this area

is necessary, and recycling strategies need to be further developed to achieve acceptable technical suitability.

Author Contributions: Conceptualization, writing—review and editing, D.F.B.d.M., S.D. and M.P.; formal analysis, investigation, writing—original draft preparation, visualization, D.F.B.d.M. and S.D.; resources, supervision, project administration, funding acquisition, M.P. All authors have read and agreed to the published version of the manuscript.

Funding: This work was supported by the Swedish Energy Agency (Energimyndigheten) under grant number P2022-00077, as well as by the Nordic 5 Tech alliance.

Data Availability Statement: Not applicable.

Acknowledgments: Crystalline structure of $LiFePO_4$ (Figure 1a) was constructed using VESTA software version 3.90.1a. Please refer to citation [16] for a proper acknowledgment, as requested by the software developers.

Conflicts of Interest: The authors declare no conflicts of interest. The funders had no role in the design of the study; in the collection, analyses, or interpretation of data; in the writing of the manuscript; or in the decision to publish the results.

References

1. Assembly, U.G. *Transforming our World: The 2030 Agenda for Sustainable Development*; United Nations: New York, NY, USA, 2020; A/RES/70/1.
2. Whittingham, M.S. History, evolution, and future status of energy storage. *Proc. IEEE* **2012**, *100*, 1518–1534. [CrossRef]
3. Mazloomi, K.; Gomes, C. Hydrogen as an energy carrier: Prospects and challenges. *Renew. Sustain. Energy Rev.* **2012**, *16*, 3024–3033. [CrossRef]
4. Chagnes, A.; Swiatowska, J. *Lithium Process Chemistry: Resources, Extraction, Batteries, and Recycling*; Elsevier: Amsterdam, The Netherlands, 2015.
5. Tarascon, J.-M.; Armand, M. Issues and challenges facing rechargeable lithium batteries. *Nature* **2001**, *414*, 359–367. [CrossRef]
6. Ramström, O. *Scientific Background on the Nobel Prize in Chemistry 2019*; The Royal Academy of Sciences: Stockholm, Sweden, 2019.
7. Bard, A.J.; Faulkner, L.R.; White, H.S. *Electrochemical Methods: Fundamentals and Applications*; John Wiley & Sons: Hoboken, NJ, USA, 2022.
8. Gong, M.; Yu, R.; Zhou, C.; Yu, Y.; Pan, Q.; Dong, C.; Shen, C.; Guan, Y.; Sun, C.; Mai, L.; et al. Mechanically robust current collector with gradient lithiophilicity induced by spontaneous lithium ion diffusion for stable lean-lithium metal batteries. *ACS Nano* **2024**, *18*, 20648–20658. [CrossRef] [PubMed]
9. Hu, J.; Huang, W.; Yang, L.; Pan, F. Structure and performance of the $LiFePO_4$ cathode material: From the bulk to the surface. *Nanoscale* **2020**, *12*, 15036–15044. [CrossRef]
10. Andersson, A.S.; Thomas, J.O.; Kalska, B.; Häggström, L. Thermal stability of $LiFePO_4$-based cathodes. *Electrochem. Solid-State Lett.* **1999**, *3*, 66. [CrossRef]
11. Padhi, A.; Nanjundaswamy, K.; Masquelier, C.; Okada, S.; Goodenough, J. Effect of structure on the Fe^{3+}/Fe^{2+} redox couple in iron phosphates. *J. Electrochem. Soc.* **1997**, *144*, 1609. [CrossRef]
12. Padhi, A.K.; Nanjundaswamy, K.S.; Goodenough, J.B. Phospho-olivines as positive-electrode materials for rechargeable lithium batteries. *J. Electrochem. Soc.* **1997**, *144*, 1188. [CrossRef]
13. Battery University. *BU-216: Summary Table of Lithium-Based Batteries*; Battery University: Durant, OK, USA, 2021.
14. Boston Consulting Group. *Batteries for Electric Cars. Challenges, Opportunities, and the Outlook to 2020*; BCG Report; Boston Consulting Group: Boston, MA, USA, 2010.
15. Yang, S.; Song, Y.; Zavalij, P.Y.; Whittingham, M.S. Reactivity, stability and electrochemical behavior of lithium iron phosphates. *Electrochem. Commun.* **2002**, *4*, 239–244. [CrossRef]
16. Wang, J.; Sun, X. Olivine $LiFePO_4$: The remaining challenges for future energy storage. *Energy Environ. Sci.* **2015**, *8*, 1110–1138. [CrossRef]
17. Momma, K.; Izumi, F. VESTA 3 for three-dimensional visualization of crystal, volumetric and morphology data. *J. Appl. Crystallogr.* **2011**, *44*, 1272–1276. [CrossRef]
18. Yamada, A.; Chung, S.-C.; Hinokuma, K. Optimized $LiFePO_4$ for lithium battery cathodes. *J. Electrochem. Soc.* **2001**, *148*, A224. [CrossRef]

19. Jugović, D.; Uskoković, D. A review of recent developments in the synthesis procedures of lithium iron phosphate powders. *J. Power Sources* **2009**, *190*, 538–544. [CrossRef]
20. Yoshino, A. The birth of the lithium-ion battery. *Angew. Chem. Int. Ed.* **2012**, *51*, 5798–5800. [CrossRef] [PubMed]
21. Gaberscek, M.; Bele, M.; Drofenik, J.; Dominko, R.; Pejovnik, S. Improved carbon anode for lithium batteries pretreatment of carbon particles in a polyelectrolyte solution. *Electrochem. Solid-State Lett.* **2000**, *3*, 171. [CrossRef]
22. Asenbauer, J.; Eisenmann, T.; Kuenzel, M.; Kazzazi, A.; Chen, Z.; Bresser, D. The success story of graphite as a lithium-ion anode material–fundamentals, remaining challenges, and recent developments including silicon (oxide) composites. *Sustain. Energy Fuels* **2020**, *4*, 5387–5416. [CrossRef]
23. Schmuch, R.; Wagner, R.; Hörpel, G.; Placke, T.; Winter, M. Performance and cost of materials for lithium-based rechargeable automotive batteries. *Nat. Energy* **2018**, *3*, 267–278. [CrossRef]
24. Drofenik, J.; Gaberscek, M.; Dominko, R.; Poulsen, F.W.; Mogensen, M.; Pejovnik, S.; Jamnik, J. Cellulose as a binding material in graphitic anodes for Li ion batteries: A performance and degradation study. *Electrochim. Acta* **2003**, *48*, 883–889. [CrossRef]
25. Neumann, J.; Petranikova, M.; Meeus, M.; Gamarra, J.D.; Younesi, R.; Winter, M.; Nowak, S. Recycling of lithium-ion batteries—Current state of the art, circular economy, and next generation recycling. *Adv. Energy Mater.* **2022**, *12*, 2102917. [CrossRef]
26. Vasconcelos, D.d.S.; Tenório, J.A.S.; Junior, A.B.B.; Espinosa, D.C.R. Circular recycling strategies for LFP batteries: A review focusing on hydrometallurgy sustainable processing. *Metals* **2023**, *13*, 543. [CrossRef]
27. Zhang, S.; Xu, K.; Jow, T. Low temperature performance of graphite electrode in Li-ion cells. *Electrochim. Acta* **2002**, *48*, 241–246. [CrossRef]
28. Wang, F.; Chen, J.; Tan, Z.; Wu, M.; Yi, B.; Su, W.; Wei, Z.; Liu, S. Low-temperature electrochemical performances of $LiFePO_4$ cathode materials for lithium ion batteries. *J. Taiwan Inst. Chem. Eng.* **2014**, *45*, 1321–1330. [CrossRef]
29. Chen, X.; Gong, Y.; Li, X.; Zhan, F.; Liu, X.; Ma, J. Perspective on low-temperature electrolytes for $LiFePO_4$-based lithium-ion batteries. *Int. J. Miner. Metall. Mater.* **2023**, *30*, 1–13. [CrossRef]
30. Walvekar, H.; Beltran, H.; Sripad, S.; Pecht, M. Implications of the electric vehicle manufacturers' decision to mass adopt lithium-iron phosphate batteries. *IEEE Access* **2022**, *10*, 63834–63843. [CrossRef]
31. Fernholm, A. *They Developed the World's Most Powerful Battery*; The Royal Swedsh Academy of Sciences: Stockholm, Sweden, 2019.
32. Latini, D.; Vaccari, M.; Lagnoni, M.; Orefice, M.; Mathieux, F.; Huisman, J.; Tognotti, L.; Bertei, A. A comprehensive review and classification of unit operations with assessment of outputs quality in lithium-ion battery recycling. *J. Power Sources* **2022**, *546*, 231979. [CrossRef]
33. Zhang, P.; Yokoyama, T.; Itabashi, O.; Suzuki, T.M.; Inoue, K. Hydrometallurgical process for recovery of metal values from spent lithium-ion secondary batteries. *Hydrometallurgy* **1998**, *47*, 259–271. [CrossRef]
34. Kim, H.S.; Shin, E.J. Re-synthesis and electrochemical characteristics of $LiFePO_4$ cathode materials recycled from scrap electrodes. *Bull. Korean Chem. Soc.* **2013**, *34*, 851–855. [CrossRef]
35. Bergfald, B.; Kristensen, K.; Lystad, H. *Recycling of Critical Raw Materials in the Nordics*; Nordisk Ministerråd: Copenhagen, Denmark, 2024.
36. European Union. *Regulation (EU) 2023/1542 of the European Parliament and of the Council of 12 July 2023 Concerning Batteries and Waste Batteries, Amending Directive 2008/98/EC and Regulation (EU) 2019/1020 and Repealing Directive 2006/66/EC: Regulation (EU) 2023/1542*; European Union: Brussels, Belgium, 2023.
37. Neubauer, J.; Pesaran, A. The ability of battery second use strategies to impact plug-in electric vehicle prices and serve utility energy storage applications. *J. Power Sources* **2011**, *196*, 10351–10358. [CrossRef]
38. Enache, B.-A.; Seritan, G.-C.; Cepisca, C.; Grigorescu, S.-D.; Argatu, F.-C.; Adochiei, F.-C.; Voicila, T.I. Comparative study of screening methods for second life $LiFePO_4$ batteries. *Screening* **2020**, *5*, 14.
39. Wang, Y.; Tang, B.; Shen, M.; Wu, Y.; Qu, S.; Hu, Y.; Feng, Y. Environmental impact assessment of second life and recycling for $LiFePO_4$ power batteries in China. *J. Environ. Manag.* **2022**, *314*, 115083. [CrossRef] [PubMed]
40. Koch-Ciobotaru, C.; Saez-de-Ibarra, A.; Martinez-Laserna, E.; Stroe, D.-I.; Swierczynski, M.; Rodriguez, P. Second life battery energy storage system for enhancing renewable energy grid integration. In Proceedings of the 2015 IEEE Energy Conversion Congress and Exposition (ECCE), Montreal, QC, Canada, 20–24 September 2015; IEEE: Piscataway, NJ, USA, 2015.
41. Illa Font, C.H.; Siqueira, H.V.; Neto, J.E.M.; Santos, J.L.F.D.; Stevan, S.L., Jr.; Converti, A.; Corrêa, F.C. Second life of lithium-ion batteries of electric vehicles: A short review and perspectives. *Energies* **2023**, *16*, 953. [CrossRef]
42. Mukhopadhyay, A.; Sheldon, B.W. Deformation and stress in electrode materials for Li-ion batteries. *Prog. Mater. Sci.* **2014**, *63*, 58–116. [CrossRef]
43. Nagpure, S.C.; Bhushan, B.; Babu, S.; Rizzoni, G. Scanning spreading resistance characterization of aged Li-ion batteries using atomic force microscopy. *Scr. Mater.* **2009**, *60*, 933–936. [CrossRef]
44. Zhang, J.; Yu, H.; Zhang, X.; Xia, M.; Zhang, X.; Zhang, L.; Shui, M.; Cui, Y.; Shu, J. Surface chemistry of $LiFePO_4$ cathode material as unraveled by HRTEM and XPS. *Ionics* **2021**, *27*, 31–37. [CrossRef]

45. Agubra, V.A.; Fergus, J.W. The formation and stability of the solid electrolyte interface on the graphite anode. *J. Power Sources* **2014**, *268*, 153–162. [CrossRef]
46. Meda, U.S.; Lal, L.; Sushantha, M.; Garg, P. Solid Electrolyte Interphase (SEI), a boon or a bane for lithium batteries: A review on the recent advances. *J. Energy Storage* **2022**, *47*, 103564. [CrossRef]
47. Köbbing, L.; Latz, A.; Horstmann, B. Growth of the solid-electrolyte interphase: Electron diffusion versus solvent diffusion. *J. Power Sources* **2023**, *561*, 232651. [CrossRef]
48. Gachot, G.; Grugeon, S.; Armand, M.; Pilard, S.; Guenot, P.; Tarascon, J.-M.; Laruelle, S. Deciphering the multi-step degradation mechanisms of carbonate-based electrolyte in Li batteries. *J. Power Sources* **2008**, *178*, 409–421. [CrossRef]
49. Demirocak, D.E.; Bhushan, B. Probing the aging effects on nanomechanical properties of a $LiFePO_4$ cathode in a large format prismatic cell. *J. Power Sources* **2015**, *280*, 256–262. [CrossRef]
50. Sharifi-Asl, S.; Lu, J.; Amine, K.; Shahbazian-Yassar, R. Oxygen release degradation in Li-ion battery cathode materials: Mechanisms and mitigating approaches. *Adv. Energy Mater.* **2019**, *9*, 1900551. [CrossRef]
51. Hu, L.-H.; Wu, F.-Y.; Lin, C.-T.; Khlobystov, A.N.; Li, L.-J. Graphene-modified $LiFePO_4$ cathode for lithium ion battery beyond theoretical capacity. *Nat. Commun.* **2013**, *4*, 1687. [CrossRef] [PubMed]
52. Kumar, J.; Shen, X.; Li, B.; Liu, H.; Zhao, J. Selective recovery of Li and FePO4 from spent $LiFePO_4$ cathode scraps by organic acids and the properties of the regenerated $LiFePO_4$. *Waste Manag.* **2020**, *113*, 32–40. [CrossRef]
53. Yan, K.; Chen, Q.; Zhang, Z.; Nie, H.; Wang, R.; Xu, Z. A closed-loop process for high-value regeneration of spent $LiFePO_4$ cathodes after selective aluminium precipitation. *Green Chem.* **2023**, *25*, 9156–9166. [CrossRef]
54. Liu, K.; Wang, J.; Wang, M.; Zhang, Q.; Cao, Y.; Huang, L.; Valix, M.; Tsang, D.C. Low-carbon recycling of spent lithium iron phosphate batteries via a hydro-oxygen repair route. *Green Chem.* **2023**, *25*, 6642–6651. [CrossRef]
55. Jin, H.; Zhang, J.; Wang, D.; Jing, Q.; Chen, Y.; Wang, C. Facile and efficient recovery of lithium from spent $LiFePO_4$ batteries via air oxidation–water leaching at room temperature. *Green Chem.* **2022**, *24*, 152–162. [CrossRef]
56. Wang, P.; Lou, X.; Chen, Q.; Liu, Y.; Sun, X.; Guo, Y.; Zhang, X.; Wang, R.; Wang, Z.; Chen, S. Spent $LiFePO_4$: An old but vigorous peroxymonosulfate activator for degradation of organic pollutants in water. *Environ. Res.* **2022**, *214*, 113780. [CrossRef] [PubMed]
57. Li, Z.J.; Ali, G.; Kim, H.J.; Yoo, S.H.; Cho, S.O. $LiFePO_4$ microcrystals as an efficient heterogeneous Fenton-like catalyst in degradation of rhodamine 6G. *Nanoscale Res. Lett.* **2014**, *9*, 1–7. [CrossRef] [PubMed]
58. Zhou, J.; Jia, Q.; Wang, L.; Zhao, Y.; Ma, X.; Gong, L.; Zhang, H.; Zuo, T. Highly efficient and selective photocatalytic CO_2 reduction using MIL-125 (Ti) and based on $LiFePO_4$ and CuO QDs surface–interface regulation. *Catal. Sci. Technol.* **2022**, *12*, 5152–5161. [CrossRef]
59. Yue, X.-H.; Zhang, C.-C.; Zhang, W.-B.; Wang, Y.; Zhang, F.-S. Recycling phosphorus from spent $LiFePO_4$ battery for multifunctional slow-release fertilizer preparation and simultaneous recovery of Lithium. *Chem. Eng. J.* **2021**, *426*, 131311. [CrossRef]
60. Nasser, O.A.; Petranikova, M. Review of achieved purities after li-ion batteries hydrometallurgical treatment and impurities effects on the cathode performance. *Batteries* **2021**, *7*, 60. [CrossRef]
61. Kaas, A.; Wilke, C.; Vanderbruggen, A.; Peuker, U.A. Influence of different discharge levels on the mechanical recycling efficiency of lithium-ion batteries. *Waste Manag.* **2023**, *172*, 1–10. [CrossRef] [PubMed]
62. Ekberg, C.; Petranikova, M. Lithium batteries recycling. In *Lithium Process Chemistry*; Elsevier: Amsterdam, The Netherlands, 2015; pp. 233–267.
63. Bae, H.; Kim, Y. Technologies of lithium recycling from waste lithium ion batteries: A review. *Mater. Adv.* **2021**, *2*, 3234–3250. [CrossRef]
64. Wu, L.; Zhang, F.-S.; He, K.; Zhang, Z.-Y.; Zhang, C.-C. Avoiding thermal runaway during spent lithium-ion battery recycling: A comprehensive assessment and a new approach for battery discharge. *J. Clean. Prod.* **2022**, *380*, 135045. [CrossRef]
65. Ojanen, S.; Lundström, M.; Santasalo-Aarnio, A.; Serna-Guerrero, R. Challenging the concept of electrochemical discharge using salt solutions for lithium-ion batteries recycling. *Waste Manag.* **2018**, *76*, 242–249. [CrossRef] [PubMed]
66. Punt, T.; Bradshaw, S.M.; van Wyk, P.; Akdogan, G. The efficiency of black mass preparation by discharge and alkaline leaching for LIB recycling. *Minerals* **2022**, *12*, 753. [CrossRef]
67. Lee, J.; Park, S.; Jeong, S.; Park, J.; Kim, W.; Ko, G.; Park, K.; Kim, H.-I.; Kwon, K. Resynthesis of Ni-rich $Li[Ni_{0.9}Co_{0.05}Mn_{0.05}]O_2$ in simulated Li-ion battery leachate after saline discharge. *J. Alloys Compd.* **2023**, *960*, 170910. [CrossRef]
68. Wu, L.; Zhang, F.-S.; Zhang, Z.-Y.; Zhang, C.-C. Corrosion behavior and corrosion inhibition performance of spent lithium-ion battery during discharge. *Sep. Purif. Technol.* **2023**, *306*, 122640. [CrossRef]
69. Fang, Z.; Duan, Q.; Peng, Q.; Wei, Z.; Cao, H.; Sun, J.; Wang, Q. Comparative study of chemical discharge strategy to pretreat spent lithium-ion batteries for safe, efficient, and environmentally friendly recycling. *J. Clean. Prod.* **2022**, *359*, 132116. [CrossRef]
70. Sonoc, A.; Jeswiet, J.; Soo, V.K. Opportunities to improve recycling of automotive lithium ion batteries. *Procedia Cirp* **2015**, *29*, 752–757. [CrossRef]

71. Zhao, T.; Marthi, R.; Mahandra, H.; Chae, S.; Traversy, M.; Sadri, F.; Choi, Y.; Ghahreman, A. Direct selective leaching of lithium from industrial-grade black mass of waste lithium-ion batteries containing $LiFePO_4$ cathodes. *Waste Manag.* **2023**, *171*, 134–142. [CrossRef] [PubMed]
72. Lim, J.N.; Lim, G.J.; Cai, Y.; Chua, R.; Guo, Y.; Yan, Y.; Srinivasan, M. Electrolyte designs for safer lithium-ion and lithium-metal batteries. *J. Mater. Chem. A* **2023**, *11*, 22688–22717. [CrossRef]
73. Zachmann, N.; Fox, R.V.; Petranikova, M.; Ebin, B. Implementation of a sub-and supercritical carbon dioxide process for the selective recycling of the electrolyte from spent Li-ion battery. *J. CO_2 Util.* **2024**, *81*, 102703. [CrossRef]
74. Botte, G.G.; White, R.E.; Zhang, Z. Thermal stability of LiPF6–EC: EMC electrolyte for lithium ion batteries. *J. Power Sources* **2001**, *97*, 570–575. [CrossRef]
75. Gnanaraj, J.; Zinigrad, E.; Asraf, L.; Gottlieb, H.; Sprecher, M.; Schmidt, M.; Geissler, W.; Aurbach, D. A detailed investigation of the thermal reactions of LiPF6 solution in organic carbonates using ARC and DSC. *J. Electrochem. Soc.* **2003**, *150*, A1533. [CrossRef]
76. Röder, P.; Baba, N.; Friedrich, K.A.; Wiemhöfer, H.-D. Impact of delithiated Li_0FePO_4 on the decomposition of $LiPF_6$-based electrolyte studied by accelerating rate calorimetry. *J. Power Sources* **2013**, *236*, 151–157. [CrossRef]
77. Shi, G.; Wang, J.; Zhang, S.; Cheng, J.; Shao, X.; Xu, Z.; Chen, X.; Xin, B. Green regeneration and high-value utilization technology of the electrolyte from spent lithium-ion batteries. *Sep. Purif. Technol.* **2024**, *335*, 126144. [CrossRef]
78. Huang, H.; Liu, C.; Sun, Z. In-situ pyrolysis based on alkaline medium removes fluorine-containing contaminants from spent lithium-ion batteries. *J. Hazard. Mater.* **2023**, *457*, 131782. [CrossRef] [PubMed]
79. Lombardo, G.; Ebin, B.; Foreman, M.R.S.J.; Steenari, B.-M.; Petranikova, M. Incineration of EV lithium-ion batteries as a pretreatment for recycling–determination of the potential formation of hazardous by-products and effects on metal compounds. *J. Hazard. Mater.* **2020**, *393*, 122372. [CrossRef]
80. Ji, Y.; Jafvert, C.T.; Zyaykina, N.N.; Zhao, F. Decomposition of PVDF to delaminate cathode materials from end-of-life lithium-ion battery cathodes. *J. Clean. Prod.* **2022**, *367*, 133112. [CrossRef]
81. Jie, Y.; Yang, S.; Li, Y.; Hu, F.; Zhao, D.; Chang, D.; Lai, Y.; Chen, Y. Waste organic compounds thermal treatment and valuable cathode materials recovery from spent $LiFePO_4$ batteries by vacuum pyrolysis. *ACS Sustain. Chem. Eng.* **2020**, *8*, 19084–19095. [CrossRef]
82. Fu, Y.; He, Y.; Qu, L.; Feng, Y.; Li, J.; Liu, J.; Zhang, G.; Xie, W. Enhancement in leaching process of lithium and cobalt from spent lithium-ion batteries using benzenesulfonic acid system. *Waste Manag.* **2019**, *88*, 191–199. [CrossRef] [PubMed]
83. Golmohammadzadeh, R.; Dimachki, Z.; Bryant, W.; Zhang, J.; Biniaz, P.; Holl, M.M.B.; Pozo-Gonzalo, C.; Banerjee, P.C. Removal of polyvinylidene fluoride binder and other organics for enhancing the leaching efficiency of lithium and cobalt from black mass. *J. Environ. Manag.* **2023**, *343*, 118205. [CrossRef] [PubMed]
84. Sarkar, A.; May, R.; Ramesh, S.; Chang, W.; Marbella, L.E. Recovery and reuse of composite cathode binder in lithium ion batteries. *ChemistryOpen* **2021**, *10*, 545–552. [CrossRef]
85. He, K.; Zhang, Z.-Y.; Zhang, F.-S. Selectively peeling of spent $LiFePO_4$ cathode by destruction of crystal structure and binder matrix for efficient recycling of spent battery materials. *J. Hazard. Mater.* **2020**, *386*, 121633. [CrossRef] [PubMed]
86. Liu, Y.; Mu, D.; Li, R.; Ma, Q.; Zheng, R.; Dai, C. Purification and characterization of reclaimed electrolytes from spent lithium-ion batteries. *J. Phys. Chem. C* **2017**, *121*, 4181–4187. [CrossRef]
87. Fu, Y.; Schuster, J.; Petranikova, M.; Ebin, B. Innovative recycling of organic binders from electric vehicle lithium-ion batteries by supercritical carbon dioxide extraction. *Resour. Conserv. Recycl.* **2021**, *172*, 105666. [CrossRef]
88. Chen, X.; Li, S.; Wu, X.; Zhou, T.; Ma, H. In-situ recycling of coating materials and Al foils from spent lithium ion batteries by ultrasonic-assisted acid scrubbing. *J. Clean. Prod.* **2020**, *258*, 120943. [CrossRef]
89. Chen, Y.; Wang, L.; Li, J.; Tao, S.; Gan, Q.; Tang, X. Effect of Cu impurity on the electrochemical performance of regenerated $LiFePO_4$/C electrode materials. *J. Mater. Sci. Mater. Electron.* **2020**, *31*, 10460–10469. [CrossRef]
90. Zhang, L.; Zeng, D. Aluminium behaviour in preparation process of lithium iron phosphate and its effects on material electrochemical performance. *J. Mater. Res. Technol.* **2021**, *15*, 3575–3584. [CrossRef]
91. Bi, H.; Zhu, H.; Zu, L.; He, S.; Gao, Y.; Peng, J. Combined mechanical process recycling technology for recovering copper and aluminium components of spent lithium-iron phosphate batteries. *Waste Manag. Res.* **2019**, *37*, 767–780. [CrossRef]
92. Zhu, H.; Bai, Y.; Zu, L.; Bi, H.; Wen, J. Separation of metal and cathode materials from waste lithium iron phosphate battery by electrostatic process. *Separations* **2023**, *10*, 220. [CrossRef]
93. Zhong, X.; Liu, W.; Han, J.; Jiao, F.; Qin, W.; Liu, T.; Zhao, C. Pyrolysis and physical separation for the recovery of spent $LiFePO_4$ batteries. *Waste Manag.* **2019**, *89*, 83–93. [CrossRef] [PubMed]
94. Zhang, G.; He, Y.; Feng, Y.; Wang, H.; Zhang, T.; Xie, W.; Zhu, X. Enhancement in liberation of electrode materials derived from spent lithium-ion battery by pyrolysis. *J. Clean. Prod.* **2018**, *199*, 62–68. [CrossRef]
95. Hanisch, C.; Loellhoeffel, T.; Diekmann, J.; Markley, K.J.; Haselrieder, W.; Kwade, A. Recycling of lithium-ion batteries: A novel method to separate coating and foil of electrodes. *J. Clean. Prod.* **2015**, *108*, 301–311. [CrossRef]

96. Jiang, Z.; Sun, J.; Jia, P.; Wang, W.; Song, Z.; Zhao, X.; Mao, Y. A sustainable strategy for spent Li-ion battery regeneration: Microwave-hydrothermal relithiation complemented with anode-revived graphene to construct a $LiFePO_4$/MWrGO cathode material. *Sustain. Energy Fuels* **2022**, *6*, 2207–2222. [CrossRef]
97. Jia, K.; Ma, J.; Wang, J.; Liang, Z.; Ji, G.; Piao, Z.; Gao, R.; Zhu, Y.; Zhuang, Z.; Zhou, G. Long-life regenerated $LiFePO_4$ from spent cathode by elevating the d-band center of Fe. *Adv. Mater.* **2023**, *35*, 2208034. [CrossRef] [PubMed]
98. Bruno, M.; Francia, C.; Fiore, S. Closed-loop recycling of lithium iron phosphate cathodic powders via citric acid leaching. *Environ. Sci. Pollut. Res.* **2024**, 1–16. [CrossRef]
99. Qi, C.; Wang, S.; Zhu, X.; Zhang, T.; Gou, Y.; Xie, Z.; Jin, Y.; Wang, Y.; Song, L.; Zhang, M. Environmental-friendly low-cost direct regeneration of cathode material from spent $LiFePO_4$. *J. Alloys Compd.* **2022**, *924*, 166612. [CrossRef]
100. Gratz, E.; Sa, Q.; Apelian, D.; Wang, Y. A closed loop process for recycling spent lithium ion batteries. *J. Power Sources* **2014**, *262*, 255–262. [CrossRef]
101. Wu, Y.; Zhou, K.; Zhang, X.; Peng, C.; Jiang, Y.; Chen, W. Aluminum separation by sulfuric acid leaching-solvent extraction from Al-bearing $LiFePO_4$/C powder for recycling of Fe/P. *Waste Manag.* **2022**, *144*, 303–312. [CrossRef] [PubMed]
102. Sun, J.; Jiang, Z.; Jia, P.; Li, S.; Wang, W.; Song, Z.; Mao, Y.; Zhao, X.; Zhou, B. A sustainable revival process for defective $LiFePO_4$ cathodes through the synergy of defect-targeted healing and in-situ construction of 3D-interconnected porous carbon networks. *Waste Manag.* **2023**, *158*, 125–135. [CrossRef] [PubMed]
103. Wang, X.; Wang, X.; Zhang, R.; Wang, Y.; Shu, H. Hydrothermal preparation and performance of $LiFePO_4$ by using Li_3PO_4 recovered from spent cathode scraps as Li source. *Waste Manag.* **2018**, *78*, 208–216. [CrossRef] [PubMed]
104. Liu, X.; Wang, M.; Deng, L.; Cheng, Y.-J.; Gao, J.; Xia, Y. Direct regeneration of spent lithium iron phosphate via a low-temperature molten salt process coupled with a reductive environment. *Ind. Eng. Chem. Res.* **2022**, *61*, 3831–3839. [CrossRef]
105. Bai, Y.; Zhu, H.; Zu, L.; Zhang, Y.; Bi, H. Environment-friendly, efficient process for mechanical recovery of waste lithium iron phosphate batteries. *Waste Manag. Res.* **2023**, *41*, 1549–1558. [CrossRef] [PubMed]
106. Wang, H.; Liu, J.; Bai, X.; Wang, S.; Yang, D.; Fu, Y.; He, Y. Separation of the cathode materials from the Al foil in spent lithium-ion batteries by cryogenic grinding. *Waste Manag.* **2019**, *91*, 89–98. [CrossRef] [PubMed]
107. Chen, X.; Li, S.; Wang, Y.; Jiang, Y.; Tan, X.; Han, W.; Wang, S. Recycling of $LiFePO_4$ cathode materials from spent lithium-ion batteries through ultrasound-assisted Fenton reaction and lithium compensation. *Waste Manag.* **2021**, *136*, 67–75. [CrossRef] [PubMed]
108. Yao, T.; Zhang, H.; Qi, C.; Ma, J.; Zhou, Z.; Sun, Q.; Song, L.; Jin, Y.; Zhang, M. Effective regeneration of waste $LiFePO_4$ cathode material by Cu doping modification. *Appl. Surf. Sci.* **2024**, *659*, 159920. [CrossRef]
109. Song, L.; Qi, C.; Wang, S.; Zhu, X.; Zhang, T.; Jin, Y.; Zhang, M. Direct regeneration of waste $LiFePO_4$ cathode materials with a solid-phase method promoted by activated CNTs. *Waste Manag.* **2023**, *157*, 141–148. [CrossRef] [PubMed]
110. Zhao, Y.; Fang, L.-Z.; Kang, Y.-Q.; Wang, L.; Zhou, Y.-N.; Liu, X.-Y.; Li, T.; Li, Y.-X.; Liang, Z.; Zhang, Z.-X.; et al. A novel three-step approach to separate cathode components for lithium-ion battery recycling. *Rare Met.* **2021**, *40*, 1431–1436. [CrossRef]
111. Xu, P.; Dai, Q.; Gao, H.; Liu, H.; Zhang, M.; Li, M.; Chen, Y.; An, K.; Meng, Y.; Liu, P. Efficient direct recycling of lithium-ion battery cathodes by targeted healing. *Joule* **2020**, *4*, 2609–2626. [CrossRef]
112. Song, X.; Hu, T.; Liang, C.; Long, H.; Zhou, L.; Song, W.; You, L.; Wu, Z.; Liu, J. Direct regeneration of cathode materials from spent lithium iron phosphate batteries using a solid phase sintering method. *RSC Adv.* **2017**, *7*, 4783–4790. [CrossRef]
113. Wang, M.; Tan, Q.; Liu, L.; Li, J. Revealing the dissolution mechanism of polyvinylidene fluoride of spent lithium-ion batteries in waste oil-based methyl ester solvent. *ACS Sustain. Chem. Eng.* **2020**, *8*, 7489–7496. [CrossRef]
114. Fan, X.; Song, C.; Lu, X.; Shi, Y.; Yang, S.; Zheng, F.; Huang, Y.; Liu, K.; Wang, H.; Li, Q. Separation and recovery of valuable metals from spent lithium-ion batteries via concentrated sulfuric acid leaching and regeneration of $LiNi_{1/3}Co_{1/3}Mn_{1/3}O_2$. *J. Alloys Compd.* **2021**, *863*, 158775. [CrossRef]
115. Chen, Z.; Feng, R.; Wang, W.; Tu, S.; Hu, Y.; Wang, X.; Zhan, R.; Wang, J.; Zhao, J.; Liu, S. Reaction-passivation mechanism driven materials separation for recycling of spent lithium-ion batteries. *Nat. Commun.* **2023**, *14*, 4648. [CrossRef] [PubMed]
116. Bai, Y.; Muralidharan, N.; Li, J.; Essehli, R.; Belharouak, I. Sustainable direct recycling of lithium-ion batteries via solvent recovery of electrode materials. *ChemSusChem* **2020**, *13*, 5664–5670. [CrossRef]
117. Kong, Y.; Yuan, L.; Liao, Y.; Shao, Y.; Hao, S.; Huang, Y. Efficient separation and selective Li recycling of spent $LiFePO_4$ cathode. *Energy Mater.* **2023**, *3*, 300053. [CrossRef]
118. Cuesta, N.; Ramos, A.; Cameán, I.; Antuña, C.; García, A.B. Hydrocolloids as binders for graphite anodes of lithium-ion batteries. *Electrochim. Acta* **2015**, *155*, 140–147. [CrossRef]
119. Baboo, J.P.; Yatoo, M.A.; Dent, M.; Najafabadi, E.H.; Lekakou, C.; Slade, R.; Hinder, S.J.; Watts, J.F. Exploring different binders for a $LiFePO_4$ battery, battery testing, modeling and simulations. *Energies* **2022**, *15*, 2332. [CrossRef]
120. Thompson, D.L.; Hartley, J.M.; Lambert, S.M.; Shiref, M.; Harper, G.D.; Kendrick, E.; Anderson, P.; Ryder, K.S.; Gaines, L.; Abbott, A.P. The importance of design in lithium ion battery recycling–a critical review. *Green Chem.* **2020**, *22*, 7585–7603. [CrossRef]

121. Bi, H.; Zhu, H.; Zu, L.; Gao, Y.; Gao, S.; Bai, Y. Environment-friendly technology for recovering cathode materials from spent lithium iron phosphate batteries. *Waste Manag. Res.* **2020**, *38*, 911–920. [CrossRef] [PubMed]
122. Verdugo, L.; Zhang, L.; Etschmann, B.; Bruckard, W.; Menacho, J.; Hoadley, A. Effect of lithium ion on the separation of electrode materials in spent lithium ion batteries using froth flotation. *Sep. Purif. Technol.* **2023**, *311*, 123241. [CrossRef]
123. Li, J.; Zhang, J.; Zhao, W.; Lu, D.; Ren, G.; Tu, Y. Application of roasting flotation technology to enrich valuable metals from spent $LiFePO_4$ batteries. *ACS Omega* **2022**, *7*, 25590–25599. [CrossRef]
124. Wang, C.; Ding, E.; Zhang, X.; Zeng, Y.; Sun, W.; Wei, Z.; Yang, Y.; Tang, H. Selective flotation separation mechanism of LFPs and graphite electrode materials using CMC as inhibitor. *J. Environ. Chem. Eng.* **2024**, *12*, 112297. [CrossRef]
125. Hu, Z.; Liu, J.; Gan, T.; Lu, D.; Wang, Y.; Zheng, X. High-intensity magnetic separation for recovery of $LiFePO_4$ and graphite from spent lithium-ion batteries. *Sep. Purif. Technol.* **2022**, *297*, 121486. [CrossRef]
126. Cornelio, A.; Zanoletti, A.; Bontempi, E. Recent progress in pyrometallurgy for the recovery of spent lithium-ion batteries: A review of state-of-the-art developments. *Curr. Opin. Green Sustain. Chem.* **2024**, *46*, 100881. [CrossRef]
127. Makuza, B.; Tian, Q.; Guo, X.; Chattopadhyay, K.; Yu, D. Pyrometallurgical options for recycling spent lithium-ion batteries: A comprehensive review. *J. Power Sources* **2021**, *491*, 229622. [CrossRef]
128. Narzari, R.; Gogoi, B.; Geed, S.R. Pyrometallurgy: Urban mining and its future implications. In *Global E-Waste Management Strategies and Future Implications*; Elsevier: Amsterdam, The Netherlands, 2023; pp. 125–142.
129. Xu, Y.; Zhang, B.; Ge, Z.; Zhang, S.; Song, B.; Tian, Y.; Deng, W.; Zou, G.; Hou, H.; Ji, X. Advances and perspectives towards spent $LiFePO_4$ battery recycling. *J. Clean. Prod.* **2023**, *434*, 140077. [CrossRef]
130. Zhang, J. Pyrometallurgy-based applications in spent lithium-ion battery recycling. In *Nano Technology for Battery Recycling, Remanufacturing, and Reusing*; Elsevier: Amsterdam, The Netherlands, 2022; pp. 171–182.
131. Holzer, A.; Windisch-Kern, S.; Ponak, C.; Raupenstrauch, H. A novel pyrometallurgical recycling process for lithium-ion batteries and its application to the recycling of LCO and LFP. *Metals* **2021**, *11*, 149. [CrossRef]
132. Qu, G.; Yang, J.; Wang, H.; Ran, Y.; Li, B.; Wei, Y. Applicability of the reduction smelting recycling process to different types of spent lithium-ion batteries cathode materials. *Waste Manag.* **2023**, *166*, 222–232. [CrossRef] [PubMed]
133. Li, X.; Zhou, F.; Gao, S.; Zhao, J.; Wang, D.; Yin, H. NaOH-assisted low-temperature roasting to recover spent $LiFePO_4$ batteries. *Waste Manag.* **2022**, *153*, 347–354. [CrossRef] [PubMed]
134. Zhang, B.; Qu, X.; Chen, X.; Liu, D.; Zhao, Z.; Xie, H.; Wang, D.; Yin, H. A sodium salt-assisted roasting approach followed by leaching for recovering spent $LiFePO_4$ batteries. *J. Hazard. Mater.* **2022**, *424*, 127586. [CrossRef] [PubMed]
135. Kotaich, K.; Sloop, S.E. Cobalt-free batteries, a new frontier for advanced battery recycling. In Proceedings of the 2009 IEEE International Symposium on Sustainable Systems and Technology, Tempe, AZ, USA, 18–20 May 2009; IEEE: Piscataway, NJ, USA, 2009.
136. Zackrisson, M.; Avellán, L.; Orlenius, J. Life cycle assessment of lithium-ion batteries for plug-in hybrid electric vehicles—Critical issues. *J. Clean. Prod.* **2010**, *18*, 1519–1529. [CrossRef]
137. Holzer, A.; Wiszniewski, L.; Windisch-Kern, S.; Raupenstrauch, H. Optimization of a pyrometallurgical process to efficiently recover valuable metals from commercially used lithium-ion battery cathode materials LCO, NCA, NMC622, and LFP. *Metals* **2022**, *12*, 1642. [CrossRef]
138. Zheng, R.; Zhao, L.; Wang, W.; Liu, Y.; Ma, Q.; Mu, D.; Li, R.; Dai, C. Optimized Li and Fe recovery from spent lithium-ion batteries via a solution-precipitation method. *RSC Adv.* **2016**, *6*, 43613–43625. [CrossRef]
139. Li, H.; Xing, S.; Liu, Y.; Li, F.; Guo, H.; Kuang, G. Recovery of lithium, iron, and phosphorus from spent $LiFePO_4$ batteries using stoichiometric sulfuric acid leaching system. *ACS Sustain. Chem. Eng.* **2017**, *5*, 8017–8024. [CrossRef]
140. Kumar, J.; Neiber, R.R.; Park, J.; Soomro, R.A.; Greene, G.W.; Mazari, S.A.; Seo, H.Y.; Lee, J.H.; Shon, M.; Chang, D.W. Recent progress in sustainable recycling of $LiFePO_4$-type lithium-ion batteries: Strategies for highly selective lithium recovery. *Chem. Eng. J.* **2022**, *431*, 133993. [CrossRef]
141. Zhao, T.; Li, W.; Traversy, M.; Choi, Y.; Ghahreman, A.; Zhao, Z.; Zhang, C.; Zhao, W.; Song, Y. A review on the recycling of spent lithium iron phosphate batteries. *J. Environ. Manag.* **2024**, *351*, 119670. [CrossRef]
142. Shentu, H.; Xiang, B.; Cheng, Y.-J.; Dong, T.; Gao, J.; Xia, Y. A fast and efficient method for selective extraction of lithium from spent lithium iron phosphate battery. *Environ. Technol. Innov.* **2021**, *23*, 101569. [CrossRef]
143. Yang, Y.; Meng, X.; Cao, H.; Lin, X.; Liu, C.; Sun, Y.; Zhang, Y.; Sun, Z. Selective recovery of lithium from spent lithium iron phosphate batteries: A sustainable process. *Green Chem.* **2018**, *20*, 3121–3133. [CrossRef]
144. Jing, Q.; Zhang, J.; Liu, Y.; Yang, C.; Ma, B.; Chen, Y.; Wang, C. E-pH diagrams for the Li-Fe-P-H_2O system from 298 to 473 K: Thermodynamic analysis and application to the wet chemical processes of the $LiFePO_4$ cathode material. *J. Phys. Chem. C* **2019**, *123*, 14207–14215. [CrossRef]
145. Qin, Z.; Li, X.; Shen, X.; Cheng, Y.; Wu, F.; Li, Y.; He, Z. Electrochemical selective lithium extraction and regeneration of spent lithium iron phosphate. *Waste Manag.* **2024**, *174*, 106–113. [CrossRef]

146. Zhang, B.; Xu, Y.; Silvester, D.S.; Banks, C.E.; Deng, W.; Zou, G.; Hou, H.; Ji, X. Direct regeneration of cathode materials in spent lithium-ion batteries toward closed-loop recycling and sustainability. *J. Power Sources* **2024**, *589*, 233728. [CrossRef]
147. Lan, Y.; Li, X.; Zhou, G.; Yao, W.; Cheng, H.M.; Tang, Y. Direct regenerating cathode materials from spent lithium-ion batteries. *Adv. Sci.* **2024**, *11*, 2304425. [CrossRef] [PubMed]
148. Gao, H.; Tran, D.; Chen, Z. Seeking direct cathode regeneration for more efficient lithium-ion battery recycling. *Curr. Opin. Electrochem.* **2022**, *31*, 100875. [CrossRef]
149. Wang, Z.; Xu, H.; Liu, Z.; Jin, M.; Deng, L.; Li, S.; Huang, Y. A recrystallization approach to repairing spent $LiFePO_4$ black mass. *J. Mater. Chem. A* **2023**, *11*, 9057–9065. [CrossRef]
150. Jing, Q.; Zhang, J.; Liu, Y.; Zhang, W.; Chen, Y.; Wang, C. Direct regeneration of spent $LiFePO_4$ cathode material by a green and efficient one-step hydrothermal method. *ACS Sustain. Chem. Eng.* **2020**, *8*, 17622–17628. [CrossRef]
151. Chen, J.; Li, Q.; Song, J.; Song, D.; Zhang, L.; Shi, X. Environmentally friendly recycling and effective repairing of cathode powders from spent $LiFePO_4$ batteries. *Green Chem.* **2016**, *18*, 2500–2506. [CrossRef]
152. Li, X.; Zhang, J.; Song, D.; Song, J.; Zhang, L. Direct regeneration of recycled cathode material mixture from scrapped $LiFePO_4$ batteries. *J. Power Sources* **2017**, *345*, 78–84. [CrossRef]
153. Liang, Q.; Yue, H.; Wang, S.; Yang, S.; Lam, K.-H.; Hou, X. Recycling and crystal regeneration of commercial used $LiFePO_4$ cathode materials. *Electrochim. Acta* **2020**, *330*, 135323. [CrossRef]
154. Li, X.; Zhou, Q.; Zhang, X.; Ge, M.; Zhang, H.; Yin, Y.; Yang, S.-T. High electrochemical performance recycling spent $LiFePO_4$ materials through the preoxidation regeneration strategy. *ACS Sustain. Chem. Eng.* **2023**, *11*, 14457–14466. [CrossRef]
155. Ji, G.; Wang, J.; Liang, Z.; Jia, K.; Ma, J.; Zhuang, Z.; Zhou, G.; Cheng, H.-M. Direct regeneration of degraded lithium-ion battery cathodes with a multifunctional organic lithium salt. *Nat. Commun.* **2023**, *14*, 584. [CrossRef] [PubMed]
156. Zhu, Y.; Jiao, X.; Bian, H.; Lu, X.-Y.; Zhang, Z. Direct relithiation and efficient regeneration of spent $LiFePO_4$ materials through thermochemical healing. *Ionics* **2023**, *29*, 4569–4576. [CrossRef]
157. Kim, D.-S.; Sohn, J.-S.; Lee, C.-K.; Lee, J.-H.; Han, K.-S.; Lee, Y.-I. Simultaneous separation and renovation of lithium cobalt oxide from the cathode of spent lithium ion rechargeable batteries. *J. Power Sources* **2004**, *132*, 145–149. [CrossRef]
158. Song, W.; Liu, J.; You, L.; Wang, S.; Zhou, Q.; Gao, Y.; Yin, R.; Xu, W.; Guo, Z. Re-synthesis of nano-structured $LiFePO_4$/graphene composite derived from spent lithium-ion battery for booming electric vehicle application. *J. Power Sources* **2019**, *419*, 192–202. [CrossRef]
159. Tang, X.; Wang, R.; Ren, Y.; Duan, J.; Li, J.; Li, P. Effective regeneration of scrapped $LiFePO_4$ material from spent lithium-ion batteries. *J. Mater. Sci.* **2020**, *55*, 13036–13048. [CrossRef]
160. Wu, C.; Hu, J.; Ye, L.; Su, Z.; Fang, X.; Zhu, X.; Zhuang, L.; Ai, X.; Yang, H.; Qian, J. Direct regeneration of spent Li-ion battery cathodes via chemical relithiation reaction. *ACS Sustain. Chem. Eng.* **2021**, *9*, 16384–16393. [CrossRef]
161. Ganter, M.J.; Landi, B.J.; Babbitt, C.W.; Anctil, A.; Gaustad, G. Cathode refunctionalization as a lithium ion battery recycling alternative. *J. Power Sources* **2014**, *256*, 274–280. [CrossRef]
162. Ouaneche, T.; Courty, M.; Stievano, L.; Monconduit, L.; Guéry, C.; Sougrati, M.T.; Recham, N. Room temperature efficient regeneration of spent $LiFePO_4$ by direct chemical lithiation. *J. Power Sources* **2023**, *579*, 233248. [CrossRef]
163. Xu, Y.; Zhang, B.; Ge, Z.; Wang, H.; Hong, N.; Xiao, X.; Song, B.; Zhang, Y.; Tian, Y.; Deng, W. Direct recovery of degraded $LiFePO_4$ cathode via mild chemical relithiation strategy. *Chem. Eng. J.* **2023**, *477*, 147201. [CrossRef]
164. Im, J.; Heo, K.; Kang, S.-W.; Jeong, H.; Kim, J.; Lim, J. $LiFePO_4$ synthesis using refined Li_3PO_4 from wastewater in Li-ion battery recycling process. *J. Electrochem. Soc.* **2019**, *166*, A3861. [CrossRef]
165. Wang, T.; Yu, X.; Fan, M.; Meng, Q.; Xiao, Y.; Yin, Y.-X.; Li, H.; Guo, Y.-G. Direct regeneration of spent $LiFePO_4$ via a graphite prelithiation strategy. *Chem. Commun.* **2020**, *56*, 245–248. [CrossRef]
166. Li, C.; Du, H.; Kang, Y.; Zhao, Y.; Tian, Y.; Wozny, J.; Lu, J.; Li, T.; Tavajohi, N.; Huang, M. Room-temperature direct regeneration of spent $LiFePO_4$ cathode using the external short circuit strategy. *Next Sustain.* **2023**, *1*, 100008. [CrossRef]
167. Fan, M.; Meng, Q.; Chang, X.; Gu, C.F.; Meng, X.H.; Yin, Y.X.; Li, H.; Wan, L.J.; Guo, Y.G. In situ electrochemical regeneration of degraded $LiFePO_4$ electrode with functionalized prelithiation separator. *Adv. Energy Mater.* **2022**, *12*, 2103630. [CrossRef]
168. Shin, E.J.; Kim, S.; Noh, J.-K.; Byun, D.; Chung, K.Y.; Kim, H.-S.; Cho, B.-W. A green recycling process designed for $LiFePO_4$ cathode materials for Li-ion batteries. *J. Mater. Chem. A* **2015**, *3*, 11493–11502. [CrossRef]
169. Fu, D.; Zhou, W.; Liu, J.; Zeng, S.-Z.; Wang, L.; Liu, W.; Yu, X.; Liu, X. A facile route for the efficient leaching, recovery, and regeneration of lithium and iron from waste lithium iron phosphate cathode materials. *Sep. Purif. Technol.* **2024**, *342*, 127069. [CrossRef]
170. Peng, D.; Zhang, J.; Zou, J.; Ji, G.; Ye, L.; Li, D.; Zhang, B.; Ou, X. Closed-loop regeneration of $LiFePO_4$ from spent lithium-ion batteries: A "feed three birds with one scone" strategy toward advanced cathode materials. *J. Clean. Prod.* **2021**, *316*, 128098. [CrossRef]
171. Sun, F.; Gao, M.; Jiao, W.; Qi, L.; He, Z.; Zhang, H.; Cao, Y.; Song, D.; Zhang, L. A novel acid-free leaching route of recovering Li_2CO_3 and $FePO_4$ from spent $LiFePO_4$ black powder. *J. Alloys Compd.* **2023**, *965*, 171429. [CrossRef]

172. Xu, Y.; Qiu, X.; Zhang, B.; Di, A.; Deng, W.; Zou, G.; Hou, H.; Ji, X. Start from the source: Direct treatment of a degraded $LiFePO_4$ cathode for efficient recycling of spent lithium-ion batteries. *Green Chem.* **2022**, *24*, 7448–7457. [CrossRef]
173. Hu, G.; Gong, Y.; Peng, Z.; Du, K.; Huang, M.; Wu, J.; Guan, D.; Zeng, J.; Zhang, B.; Cao, Y. Direct recycling strategy for spent lithium iron phosphate powder: An efficient and wastewater-free process. *ACS Sustain. Chem. Eng.* **2022**, *10*, 11606–11616. [CrossRef]
174. Wang, C.; Qiu, X.; Shen, G.; Chen, X.; Wang, J.; Xie, L.; Han, Q.; Zhu, L.; Li, J.; Cao, X. Driving the rapid regeneration of $LiFePO_4$ from spent lithium-ion batteries through one-pot mechanochemical activation. *Green Chem.* **2024**, *26*, 1501–1510. [CrossRef]
175. Yang, C.; Zhang, J.-L.; Jing, Q.-K.; Liu, Y.-B.; Chen, Y.-Q.; Wang, C.-Y. Recovery and regeneration of $LiFePO_4$ from spent lithium-ion batteries via a novel pretreatment process. *Int. J. Miner. Metall. Mater.* **2021**, *28*, 1478–1487. [CrossRef]
176. Song, Y.; Xie, B.; Song, S.; Lei, S.; Sun, W.; Xu, R.; Yang, Y. Regeneration of $LiFePO_4$ from spent lithium-ion batteries via a facile process featuring acid leaching and hydrothermal synthesis. *Green Chem.* **2021**, *23*, 3963–3971. [CrossRef]
177. Qin, X.; Yang, G.; Cai, F.; Jiang, B.; Chen, H.; Tan, C.; Kandasamy, S.; Kandasamy, K.; Sulaiman, M.; Su, N. Recovery and reuse of spent $LiFePO_4$ batteries. *J. New Mater. Electrochem. Syst* **2019**, *22*, 119–124. [CrossRef]
178. Bian, D.; Sun, Y.; Li, S.; Tian, Y.; Yang, Z.; Fan, X.; Zhang, W. A novel process to recycle spent $LiFePO_4$ for synthesizing $LiFePO_4$/C hierarchical microflowers. *Electrochim. Acta* **2016**, *190*, 134–140. [CrossRef]
179. Liu, K.; Yang, S.; Lai, F.; Li, Q.; Wang, H.; Tao, T.; Xiang, D.; Zhang, X. Application of $H_4P_2O_7$ as leaching acid in one-step selective recovery for metals from spent $LiFePO_4$ batteries. *Ionics* **2021**, *27*, 5127–5135. [CrossRef]
180. Chen, X.; Yuan, L.; Yan, S.; Ma, X. Self-activation of Ferro-chemistry based advanced oxidation process towards in-situ recycling of spent $LiFePO_4$ batteries. *Chem. Eng. J.* **2023**, *471*, 144343. [CrossRef]
181. Yadav, P.; Jie, C.J.; Tan, S.; Srinivasan, M. Recycling of cathode from spent lithium iron phosphate batteries. *J. Hazard. Mater.* **2020**, *399*, 123068. [CrossRef] [PubMed]
182. Chen, B.; Liu, M.; Cao, S.; Chen, G.; Guo, X.; Wang, X. Regeneration and performance of $LiFePO_4$ with Li_2CO_3 and $FePO_4$ as raw materials recovered from spent $LiFePO_4$ batteries. *Mater. Chem. Phys.* **2022**, *279*, 125750. [CrossRef]
183. Andersson, A.S.; Kalska, B.; Häggström, L.; Thomas, J.O. Lithium extraction/insertion in $LiFePO_4$: An X-ray diffraction and Mössbauer spectroscopy study. *Solid State Ion.* **2000**, *130*, 41–52. [CrossRef]
184. Sun, C.; Rajasekhara, S.; Goodenough, J.B.; Zhou, F. Monodisperse porous $LiFePO_4$ microspheres for a high power Li-ion battery cathode. *J. Am. Chem. Soc.* **2011**, *133*, 2132–2135. [CrossRef] [PubMed]
185. Takahashi, M.; Tobishima, S.; Takei, K.; Sakurai, Y. Characterization of $LiFePO_4$ as the cathode material for rechargeable lithium batteries. *J. Power Sources* **2001**, *97*, 508–511. [CrossRef]
186. Doeff, M.M.; Visco, S.J.; Yanping, M.; Peng, M.; Lei, D.; De Jonghe, L.C. Thin film solid state sodium batteries for electric vehicles. *Electrochim. Acta* **1995**, *40*, 2205–2210. [CrossRef]
187. Hwang, J.-Y.; Myung, S.-T.; Sun, Y.-K. Sodium-ion batteries: Present and future. *Chem. Soc. Rev.* **2017**, *46*, 3529–3614. [CrossRef] [PubMed]
188. Yu, T.; Li, G.; Duan, Y.; Wu, Y.; Zhang, T.; Zhao, X.; Luo, M.; Liu, Y. The research and industrialization progress and prospects of sodium ion battery. *J. Alloys Compd.* **2023**, *958*, 170486. [CrossRef]
189. Wan, G.; Dou, W.; Zhu, H.; Zhang, W.; Liu, T.; Wang, L.; Lu, J. Empowering higher energy sodium-ion battery cathode by oxygen chemistry. *Interdiscip. Mater.* **2023**, *2*, 416–422. [CrossRef]